



The Meningococcal Cysteine Transport System Plays a Crucial Role in *Neisseria meningitidis* Survival in Human Brain Microvascular Endothelial Cells

Hideyuki Takahashi,^a Haruo Watanabe,^{a,b} Kwang Sik Kim,^c Shigeyuki Yokoyama,^d Tatsuo Yanagisawa^d

^aDepartment of Bacteriology I, National Institute of Infectious Diseases, Tokyo, Japan

^bSchool of Medicine, International University of Health and Welfare, Chiba, Japan

^cDivision of Pediatric Infectious Diseases, Department of Pediatrics, School of Medicine, Johns Hopkins University, Baltimore, Maryland, USA

^dRIKEN Structural Biology Laboratory, Yokohama, Japan

ABSTRACT While *Neisseria meningitidis* typically exists in an asymptomatic nasopharyngeal carriage state, it may cause potentially lethal diseases in humans, such as septicemia or meningitis, by invading deeper sites in the body. Since the nutrient compositions of human cells are not always conducive to meningococci, *N. meningitidis* needs to exploit nutrients from host environments. In the present study, the utilization of cysteine by the meningococcal cysteine transport system (CTS) was analyzed for the pathogenesis of meningococcal infections. A *N. meningitidis* strain deficient in one of the three *cts* genes annotated as encoding cysteine-binding protein (*cbp*) exhibited approximately 100-fold less internalization into human brain microvascular endothelial cells (HBMEC) than the wild-type strain. This deficiency was restored by complementation with the three *cts* genes together, and the infectious phenotype of HBMEC internalization correlated with cysteine uptake activity. However, efficient accumulation of ezrin was observed beneath the *cbp* mutant. The intracellular survival of the *cbp* mutant in HBMEC was markedly reduced, whereas equivalent reductions of glutathione concentrations and of resistance to reactive oxygen species in the *cbp* mutant were not found. The *cbp* mutant grew well in complete medium but not in synthetic medium supplemented with less than 300 μ M cysteine. Taking cysteine concentrations in human cells and other body fluids, including blood and cerebrospinal fluid, into consideration, the present results collectively suggest that the meningococcal CTS is crucial for the acquisition of cysteine from human cells and participates in meningococcal nutrient virulence.

IMPORTANCE *Neisseria meningitidis* colonizes at a nasopharynx of human as a unique host and has many strains that are auxotrophs for amino acids for their growth. To cause invasive meningococcal diseases (IMD) such as sepsis and meningitis, *N. meningitidis* passes through epithelial and endothelial barriers and infiltrates into blood and cerebrospinal fluid as well as epithelial and endothelial cells. However, meningococcal nutrients, including cysteine, become less abundant when it more deeply infiltrates the human body even during inflammation, such that *N. meningitidis* has to acquire nutrients in order to survive/persist, disseminate, and proliferate in humans. This was the first study to examine the relationship between meningococcal cysteine acquisition and the pathogenesis of meningococcal infections. The results of the present study provide insights into the mechanisms by which pathogens with auxotrophs acquire nutrients in hosts and may also contribute to the development of treatments and prevention strategies for IMD.

KEYWORDS *Neisseria meningitidis*, blood, cerebrospinal fluid, cysteine, glutathione, internalization, intracellular growth, reactive oxygen species, serum, survival

Received 22 October 2018 Accepted 2 November 2018 Published 11 December 2018

Citation Takahashi H, Watanabe H, Kim KS, Yokoyama S, Yanagisawa T. 2018. The meningococcal cysteine transport system plays a crucial role in *Neisseria meningitidis* survival in human brain microvascular endothelial cells. mBio 9:e02332-18. <https://doi.org/10.1128/mBio.02332-18>.

Editor Kirsten Nielsen, University of Minnesota Medical School

Copyright © 2018 Takahashi et al. This is an open-access article distributed under the terms of the [Creative Commons Attribution 4.0 International license](https://creativecommons.org/licenses/by/4.0/).

Address correspondence to Hideyuki Takahashi, hideyuki@nih.go.jp.

This article is a direct contribution from a Fellow of the American Academy of Microbiology. Solicited external reviewers: David Stephens, Emory University; Christoph Schoen, University of Würzburg.

Neisseria meningitidis is a fastidious Gram-negative microorganism that generally exists in the noninvasive so-called “carrier state” at a rate of approximately 0.4% to 25% in human populations (1, 2). However, for reasons not yet fully understood, *N. meningitidis* exhibits the ability to cross the epithelial layer, infiltrate the bloodstream, evade the defenses of the human immune system, adhere to the endothelial layers of peripheral and brain vessels, cross the brain-blood barrier (BBB), and replicate in cerebrospinal fluid (CSF). While epidemiological analyses have suggested that a human genetic polymorphism (3) and environmental conditions such as smoking (4, 5) and climate conditions (6) are important for predicting the outcomes of infection, the reasons that IMD occurs in some individuals but not in others remain unclear.

Classical and recent advanced analyses such as reverse genetics have revealed so far that factors exposed to meningococcal surfaces such as the polysaccharide capsule, Opa and Opc (reviewed in references 7, 8, 9, and 10), NhhA (11), NadA (12), App (11), NalP (13), MspA (14), TspA (15), adhesion complex protein (ACP) (16), and fHbp (17) are related to the pathogenesis of the strain. However, the gene contents of meningococcal strains isolated from healthy carriers and patients with IMD were mostly indistinguishable (18), and genomic islands, which are found in pathogenic but not in nonpathogenic *Neisseria*, were not present in the meningococcal or neisserial genomes of any of the neisserial strains examined (19) or in meningococcal isolates from patients and healthy carriers (20, 21). Thus, the mechanisms by which *N. meningitidis* causes septicemia and meningitis in humans, in particular, the trigger to induce IMD from a carrier state, have not yet been elucidated (22, 23).

Meningococcal research has mainly focused on so-called “meningococcal virulence factors” that directly interact with the host components described above but do not involve microbial nutrients and metabolism in the host. However, acquisition of nutrients from human hosts appears to be important for meningococcal pathogenesis because the availability of the nutrient supply needed by facultative meningococci to cause IMD is limited in the human environment (24–26). A well-known example of the acquisition of nutrients is that of iron in humans; *N. meningitidis* robs human iron from host factors such as hemoglobin, transferrin, and lactoferrin (27). While human has as the first line of defense Fe sequestration from free Fe (called “nutrient immunity”) (28, 29), *N. meningitidis* overcomes the nutrient immunity by preparing bacterial high-affinity receptors to take iron from iron-chelating host molecules (29). Thus, metabolic adaptation in humans enables meningococci to exploit host resources, which supports the concept of bacterial “nutrient virulence” against hostile nutrient immunity as a crucial factor influencing invasive capabilities (25). Experimental data has indicated that many *N. meningitidis* strains are auxotrophs for at least 4 amino acids, namely, glutamate, cysteine, arginine, and glycine (30), and previous studies also demonstrated that glutamate uptake is required for bacterial intracellular growth/survival in human cells (31–33) as well as for survival and proliferation in mice (34, 35). Moreover, a reduced sulfur form of cysteine, cystine, was found to be necessary for meningococcal growth (36, 37), and many *N. meningitidis* strains had cysteine auxotroph for growth in the presence of low cysteine concentrations (38–40). However, the relationship between cysteine uptake and the pathogenesis of meningococcal infections currently remains unclear. The results obtained in the present study demonstrated that the uptake of cysteine by the meningococcal CTS was crucial for *N. meningitidis* survival/persistence in human endothelial cells.

RESULTS

Cysteine transport system (CTS) proteins, but not a sole Cbp protein, participated in meningococcal infections in HBMEC. The genes that participate in cysteine transport have already been assigned by genome sequencing and annotation analyses in *N. meningitidis* strain MC58 (41). In the present study, NMB0787 (amino acid ABC transporter substrate-binding protein), NMB0788 (amino acid ABC transporter permease), and NMB0789 (amino acid ABC transporter ATP-binding protein) were renamed cysteine-binding protein (*cbp*), cysteine transporter permease (*ctp*), and cysteine ATP-

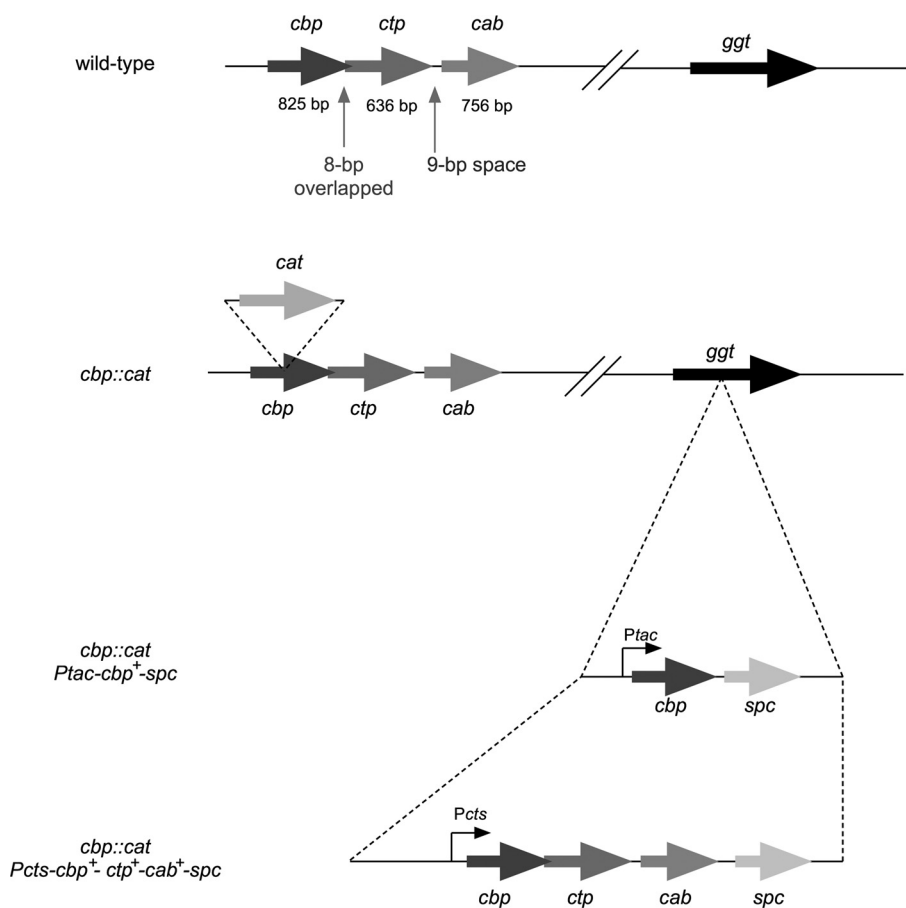


FIG 1 Schematic representation of wild-type strain and insertion mutant in the *cbp* gene and ectopic complementation of *Ptac cbp⁺* or *cbp⁺ ctp⁺ cab⁺* genes at the *ggt* locus in *N. meningitidis* strains.

binding protein (*cab*), respectively (Fig. 1) and represent the cysteine transport system (CTS). In the present study, we constructed an insertion mutation in the *cbp* gene and analyzed its biological function in meningococcal nutrient virulence.

Infectious abilities in human brain microvascular endothelial cells (HBMEC) were initially examined. The growth rate of the *cbp* mutant in assay medium (AM) (see Materials and Methods) was approximately one-third that of the wild-type strain in a 4-h incubation with shaking (data not shown). The adhesion ability of the *cbp* mutant HT1959 strain was reduced to approximately one-third that of the wild-type strain (Fig. 2A), which might reflect the growth rate difference in AM. On the other hand, the number of internalized bacteria decreased to approximately 1/100 that of wild-type strain NIID84 Δcps (*Opa⁻*, *Opc^{+/-}*) (Fig. 2B; see also Fig. S1 in the supplemental material). It was important that the same phenotype was observed in the other meningococcal strains, NIID512 (*Opa⁺*, *Opc⁻*) and NIID521 (*Opa⁺*, *Opc^{+/-}*) (Fig. 2A and B; see also Fig. S1). In order to confirm the relationship between insertional mutation and infection defects, HT 2077, a *cbp* mutant complemented with the wild-type *cbp⁺* gene expressed from the *tac* promoter in *trans* at the *ggt* locus (Fig. 1) was constructed and examined in HBMEC. It is important that the insertion of genes at the *ggt* locus did not affect meningococcal infection of human endothelial and epithelial cells (32, 33, 38, 42, 43). While the Cbp protein was expressed in HT2077 (Fig. 2D), the infectious defect was not restored in HT2077 (Fig. 2B and C). In contrast, the infectious defect in HBMEC was restored by complementation with three wild-type *cts* genes (*cbp⁺*, *ctp⁺*, and *cab⁺*) in *trans* at the *ggt* locus in the HT2080 *N. meningitidis* strain (Fig. 1 and 2B and C). It is important that the same results were again obtained in the NIID512 and NIID521 genetic backgrounds (Fig. 2). The transcription of *cts* genes in these mutants examined

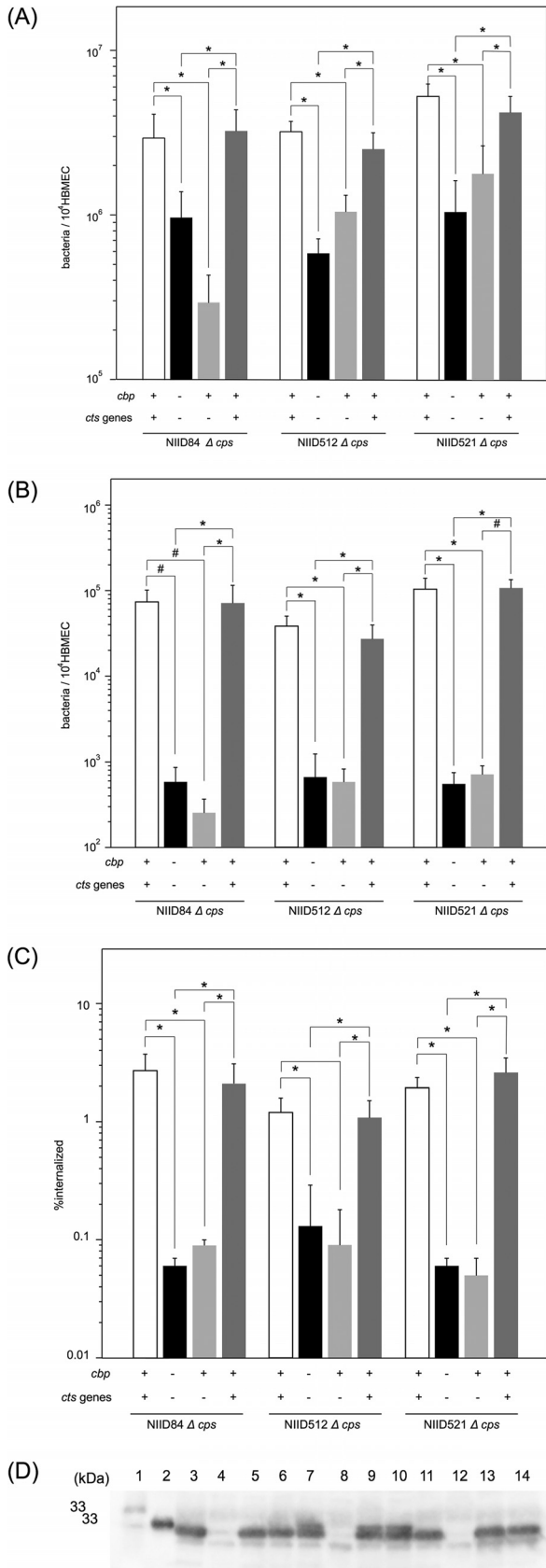


FIG 2 Mutation in *cts* genes affected apparent *N. meningitidis* internalization into HBMEC. (A to C) Adherence (A), internalization (B), and ratio of internalization/adhesion (percent internalized) (C) of *cbp* (Continued on next page)

by reverse transcriptase PCR (RT-PCR) was consistent with the infection recovery in Fig. 2; *cbp* mRNA was detected in NIID84 Δ *cps*, HT2080, and HT2077, in which only the *cbp* gene was complemented, but *ctp* and *cab* mRNA were detected only in NIID84 Δ *cps* and HT2080, indicating that the *cbp*, *ctp*, and *cab* genes were transcriptionally comprised of one operon at the *cts* gene allele (Fig. S2). Taken together, these results suggested that all three *cts* genes, but not *cbp* alone, were required for the meningococcal infection of HBMEC. Moreover, considering the expression profiles of Opa and Opc (Fig. S1), which also affect meningococcal infection of cultured human cells (44–46), these proteins could not be related to the results observed in this study.

Therefore, the subsequent experiments were performed using the NIID84 Δ *cps* strain only.

Cysteine uptake activity via the CTS correlated with the meningococcal infection of HBMEC. While all three proteins (Cbp, Ctp, and Cab) were clearly required for the efficient internalization of HBMEC, the relationship between the pathogen's infectious abilities and cysteine transport via the CTS remained unknown. Therefore, we investigated cysteine uptake activity. In our previous studies, L-glutamate uptake activity via the GltT-GltM transport system was examined in buffer A containing 20 mM NaCl for 20 s (32) because L-glutamate uptake is driven by a Na⁺ gradient (31). However, under the same conditions, [³⁵S]cysteine was imported very inefficiently into *N. meningitidis* (see Fig. 3A compared to Fig. S3A). Moreover, the addition of NaCl did not promote uptake (data not shown). Thus, in the present study, synthetic medium (SM) devoid of cysteine (see Materials and Methods) was used instead of buffer A containing NaCl. Since increases in NaCl concentrations in SM did not stimulate meningococcal cysteine uptake (Fig. S3C), meningococcal cysteine uptake was examined in SM containing 60 mM NaCl in the present study. Under these conditions, [³⁵S]cysteine was imported less efficiently in *cbp* mutant HT1959 than in wild-type strain NIID84 Δ *cps* (Fig. 3A). The low efficiency of cysteine uptake was not restored in HT2077 (a *cbp* mutant complemented with a *cbp*⁺ gene only) but recovered in the HT2080 *N. meningitidis* strain (a *cbp* mutant complemented with all three *cts*⁺ genes) (Fig. 3A). The correlation observed with infectious abilities in HBMEC (Fig. 2B and C) suggested that the efficient influx of extracellular cysteine via the CTS into *N. meningitidis* contributed to the efficient meningococcal internalization into HBMEC (see Discussion).

Ezrin accumulation was observed beneath the *cbp* *N. meningitidis* mutant. We previously demonstrated that the transient uptake of L-glutamate upon meningococcal adhesion to HBMEC triggered meningococcal internalization into HBMEC and the concomitant accumulation of ezrin beneath meningococci (33), which is a marker for the meningococcal stimulation of host cell signaling for internalization (47). In order to establish whether the same strategy is applicable to cysteine uptake, we analyzed changes in the host cell cytoskeleton upon meningococcal infection using indirect

FIG Legend (Continued)

N. meningitidis mutants to HBMEC and effects of complementation of the *cbp*⁺ or *cbp*⁺ *ctp*⁺ *cab*⁺ genes in the *cbp* mutant on bacterial infection. The numbers of bacteria were measured as CFU. Levels of internalized bacteria were determined as numbers of bacteria recovered after the gentamicin treatment. Each value represents the mean \pm standard error of mean (CFU per 10⁴ HBMEC) of results from at least four experiments. Open, filled, light gray, and dark gray bars in panels A, B, and C indicate the bacterial number of or percent internalized *N. meningitidis* *cts*⁺ strains (NIID84 Δ *cps*, NIID512 Δ *cps*, and NIID521 Δ *cps*), *cbp::cat* (HT1959, HT2056, and HT2063), and Δ *cps* mutants in which the *cbp*⁺ or *cts*⁺ (*cbp*⁺ *ctp*⁺ *cab*⁺) genes were ectopically complemented (HT2077, HT2078, and HT2079 or HT2080, HT2081, and HT2082), respectively (see Table 1). *, *P* < 0.001; #, *P* < 0.02 (significantly different from the *cts*⁺ strain or the Δ *cps* mutant complemented with *cts*⁺ genes). (D) Western blotting for Cbp proteins. Bacterial extracts equivalent to an OD₆₀₀ of 0.025 were analyzed by Western blotting. Lanes 1 and 2 represent molecular markers corresponding to 33 and 30 kDa, respectively. Lane 3, NIID84 Δ *cps* (*cts*⁺); lane 4, HT1959 (NIID84 Δ *cps* *cbp*); lane 5, HT2077 (NIID84 Δ *cps* *cbp* *ggt::cbp*⁺); lane 6, HT2080 (NIID84 Δ *cps* *cbp* *ggt::cts*⁺); lane 7, NIID512 Δ *cps* (*cts*⁺); lane 8, HT2056 (NIID512 Δ *cps* *cbp*); lane 9, HT2078 (NIID512 Δ *cps* *cbp* *ggt::cbp*⁺); lane 10, HT2081 (NIID512 Δ *cps* *cbp* *ggt::cts*⁺); lane 11, NIID521 Δ *cps* (*cts*⁺); lane 12, HT2063 (NIID521 Δ *cps* *cbp*); lane 13, HT2079 (NIID521 Δ *cps* *cbp* *ggt::cbp*⁺); lane 14, HT2082 (NIID521 Δ *cps* *cbp* *ggt::cts*⁺). The black arrow shows the Cbp protein in *N. meningitidis*.

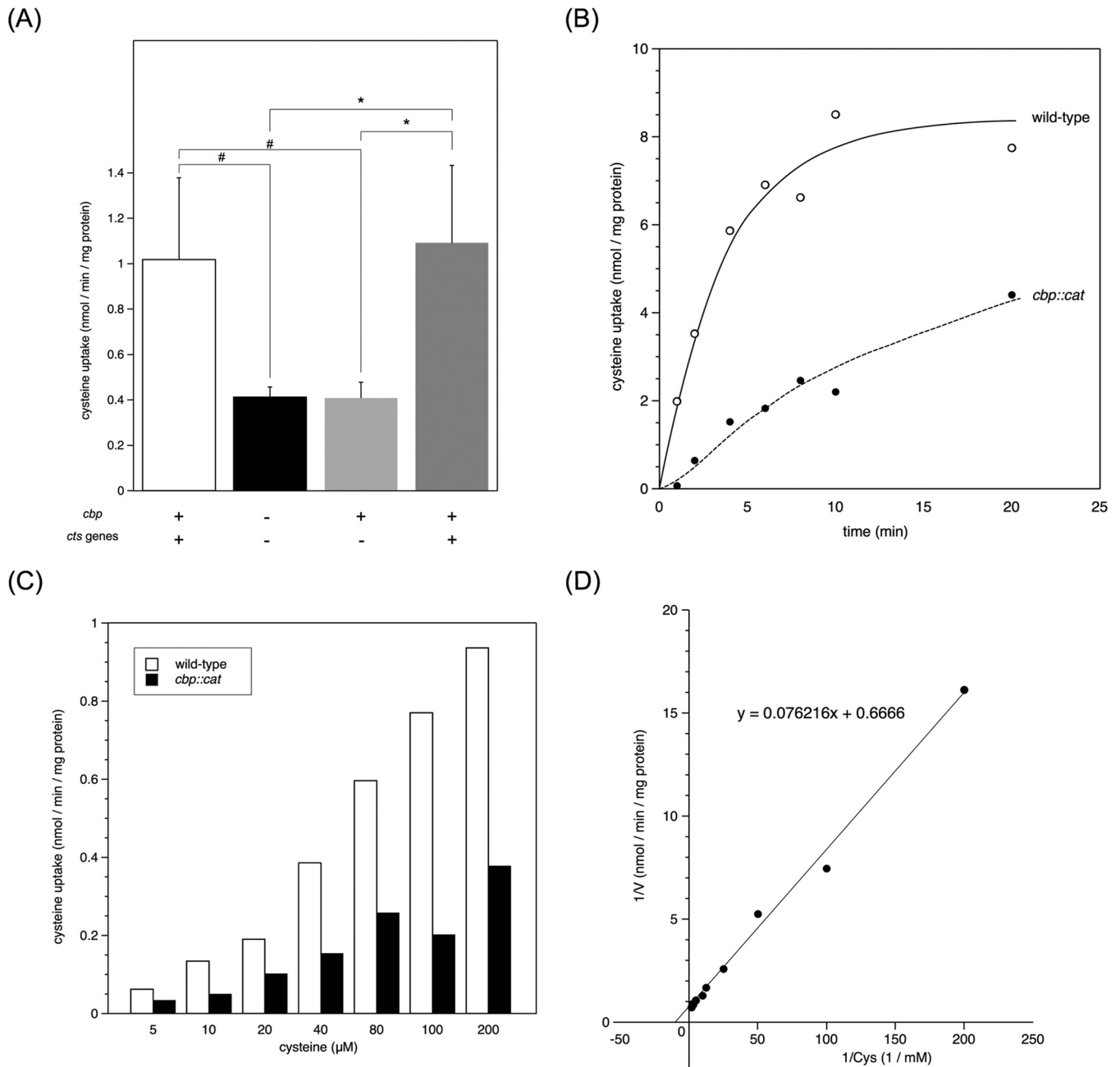


FIG 3 L-Cysteine uptake into *N. meningitidis* strains. (A) Effects of the *cbp* mutation and complementation of wild-type genes in *N. meningitidis* on L-cysteine uptake. The assay was performed as described in Materials and Methods in the presence of $100 \mu\text{M}$ L- ^{35}S cysteine and a final NaCl concentration of 60 mM in SM. Transport was examined for 5 min due to its lower efficiency than L-glutamate uptake (32). Open, filled, light gray, and dark gray bars indicate the cysteine uptake rate (nmol/min/mg protein) of NIID84 Δcps (*cts*⁺), HT1959 (NIID84 Δcps *cbp*), HT2077 (NIID84 Δcps *cbp ggt::cbp*⁺), and HT2080 (NIID84 Δcps *cbp ggt::cts*⁺), respectively. #, $P < 0.02$ (significantly different from the *cts*⁺ strain); *, $P < 0.005$ (significantly different from the Δcps *cts*⁺ strain). (B) Time course of L-cysteine uptake. The assay was performed in the presence of $100 \mu\text{M}$ L- ^{35}S cysteine and a final NaCl concentration of 60 mM in SM. The open circles with a solid line and filled circles with a dashed line indicate cysteine uptake by NIID84 Δcps (*cts*⁺) and HT1959 (NIID84 Δcps *cbp*), respectively. (C) Concentration dependence of L-cysteine import by strains NIID84 Δcps (*cts*⁺) and HT1959 (NIID84 Δcps *cbp*). The assay was performed in SM containing 60 mM NaCl for 5 min. (D) Lineweaver-Burk plot of data shown in panel C relative to NIID84 Δcps (*cts*⁺). A formula deduced from the data is also shown in the same panel. The K_m value of meningococcal ^{35}S cysteine uptake in SM was calculated to be approximately $114 \mu\text{M}$.

immunofluorescence to monitor the localization of ezrin (Fig. 4). While the accumulation of ezrin was minimal in HBMEC not infected with *N. meningitidis* (Fig. 4, left panels), it was clearly detected beneath wild-type *N. meningitidis* strain NIID84 Δcps (Fig. 4, middle panels). It is important that ezrin also accumulated beneath the *cbp* HT1959 mutant as efficiently as beneath the wild-type strain (Fig. 4, right panels), while the

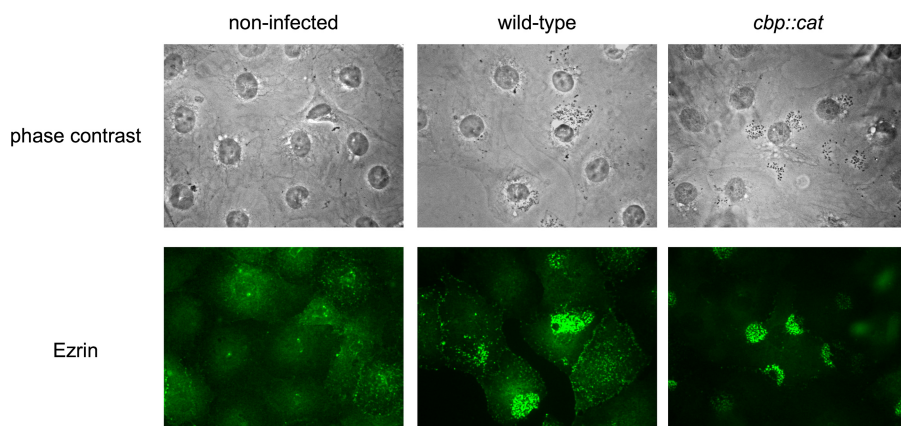


FIG 4 Immunofluorescence microscopy showing the accumulation of ezrin beneath *N. meningitidis* strains. The HBMEC monolayer was infected with wild-type *cts*⁺ (middle) and *cbp::cat* (right) *N. meningitidis* strains. A noninfected HBMEC monolayer is also shown in the left panels. Bacteria and HBMEC were observed by phase-contrast microscopy (upper panels). Ezrin was immunostained with anti-ezrin monoclonal antibodies (MAb) and Alexa Fluor 488-conjugated rabbit anti-mouse IgG (green channel) (lower panels).

ezrin accumulation was not observed in the $\Delta gltT \Delta gltM$ *N. meningitidis* strain (32, 33). This result indicated that the *cbp* mutant was not defective for stimulation of the ezrin accumulation but was defective in another mechanism(s).

The intracellular survival rate of the *cbp* mutant was reduced to the level seen with the $\Delta gshB$ mutant. Since defective L-glutamate uptake reduced glutathione synthesis and concomitantly decreased intracellular survival (31–34), it is possible that the invasion defect in the *cbp* mutant can be explained by bacterial survival/persistence in HBMEC after internalization. In order to examine this possibility, the meningococcal survival rate in HBMEC was assessed in a 4-h incubation under our experimental conditions (Fig. 5A). The intracellular bacterial number of wild-type *N. meningitidis* strain NIID84 Δcps gradually decreased during the course of the incubation, and after a 4-h incubation, approximately 60% of the bacteria remained in HBMEC (Fig. 5B). In contrast, the intracellular bacterial number of the *cbp* *N. meningitidis* mutant markedly decreased during the 4-h incubation (Fig. 5B). The rate of the decrease (6% of the zero time number) in the *cbp* mutant was markedly less than that (60% of the zero time number) of the wild-type strain. These results suggest that the *cbp* mutation decreased intracellular survival rates in HBMEC, which may have contributed to the apparent decrease in the internalized bacterial number in HBMEC (Fig. 2B).

Glutathione concentrations did not markedly decrease in the *cbp* *N. meningitidis* mutant. Previous studies reported that L-glutamate uptake is important for the synthesis of glutathione, a ubiquitous antioxidant in all living cells (48), and leads to *N. meningitidis* resistance to the neutrophil oxidative burst (34) and increased intracellular survival in human cells (31, 33). Since cysteine is also one of the components of glutathione, we constructed the *gshB* (glutathione synthetase) HT2120 mutant and examined the relationship between glutathione synthesis and the apparent ability of the *cbp* *N. meningitidis* mutant to internalize into HBMEC (Fig. 2B). While meningococcal adhesion to HBMEC was slightly affected by the *cbp* and *gshB* mutations, a marked decrease was not observed (Fig. S4A). On the other hand, the internalization of the *cbp* HT1959 mutant into HBMEC was approximately 100-fold less efficient than that of wild-type strain NIID84 Δcps , while that of the *gshB* HT2120 mutant was approximately 3-fold less efficient than that of wild-type strain NIID84 Δcps (Fig. S4B and C). These results suggest that glutathione synthesis was less likely to be related to the apparent meningococcal internalization (intracellular survival) into HBMEC.

In order to further clarify whether glutathione participates in intracellular survival, the content of glutathione was measured (Fig. 6). In *N. meningitidis* strains grown in gonococcal (GC) medium base (GCB), the intracellular glutathione concentration in the

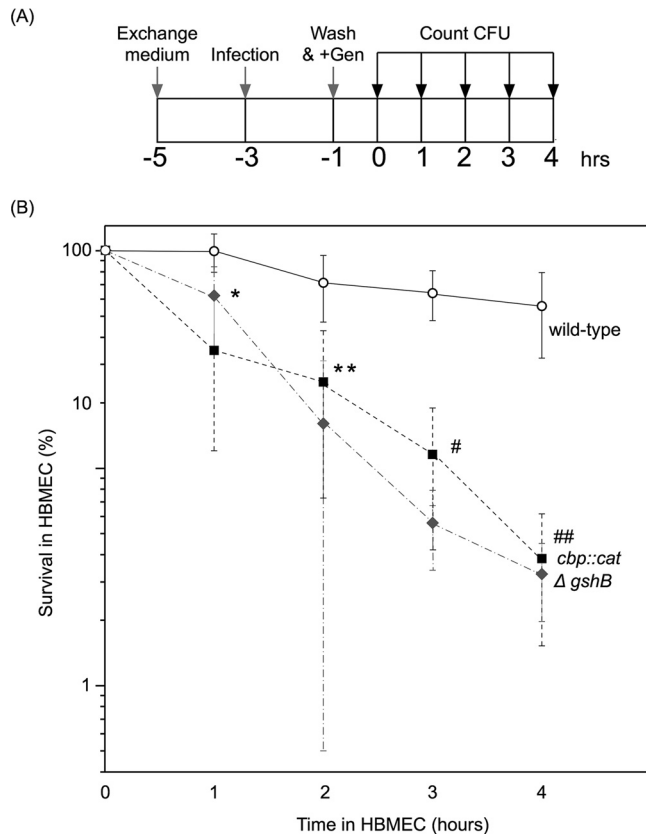


FIG 5 Percentage of survival of intracellular bacteria after killing of extracellular bacteria with gentamicin. (A) Diagram of the protocol to monitor the number of intracellular bacteria after a 2-h infection. Gen, gentamicin. Detailed procedures are described in Materials and Methods. (B) Percentage of survival of intracellular bacteria in HBMEC. Percentages of survival were calculated as $100 \times (\text{CFU at the indicated time}/\text{CFU at the removal of gentamicin})$. The open circle, filled square, and gray diamond shapes indicate the percentages of survival of *ctp*⁺ (NIID84 Δcps), *cbp::cat* (HT1959), and $\Delta gshB::spc$ (HT2120) *N. meningitidis* strains, respectively. Ranges represent mean percentages of survival in at least five experiments, and error bars represent the standard errors of the means. *, $P < 0.01$; **, $P < 0.05$; #, $P < 0.001$; ##, $P < 0.002$ (significantly different from the wild-type *cts*⁺ strain).

$\Delta gshB$ mutant was approximately 50 $\mu\text{mol}/\text{mg}$ protein, representing the background level of glutathione during the 4-h incubation (Fig. 6). Under the same conditions, wild-type *N. meningitidis* strain NIID84 Δcps had an intracellular glutathione concentration of approximately 800 $\mu\text{mol}/\text{mg}$ protein, while that in the *cbp* mutant was approximately 400 $\mu\text{mol}/\text{mg}$ protein (Fig. 6). When the strains were grown in AM, intracellular glutathione concentrations slightly decreased in the wild-type *N. meningitidis* strain but remained unchanged in the *cbp* mutant. Similar results were observed for *N. meningitidis* strains infecting HBMEC (Fig. 6). Moreover, the reduction in the glutathione amount was statistically recovered in a *cbp* mutant complemented with HT2080 *cts* genes but not in a *cbp* mutant complemented with a HT2077 *cbp* gene (Fig. S5A). These results suggest that cysteine uptake via the CTS accounts for some, but not all, of the glutathione synthesis.

Resistance to reactive oxygen species (ROS) was not largely defective in the *cbp N. meningitidis* mutant. L-Glutamate imported via GltT-GltM transporters was previously shown to be utilized in the synthesis of glutathione for resistance to H_2O_2 (34), a membrane-permeable ROS that damages proteins and DNA (49). Since glutathione concentrations were reduced to approximately 50% of the level in the wild-type strain (Fig. 6), decreases in the glutathione concentration in the *cbp* mutant may have reduced the intracellular survival rate in HBMEC. In order to examine this possibility, sensitivity to H_2O_2 and paraquat, which also generates toxic oxygen species during

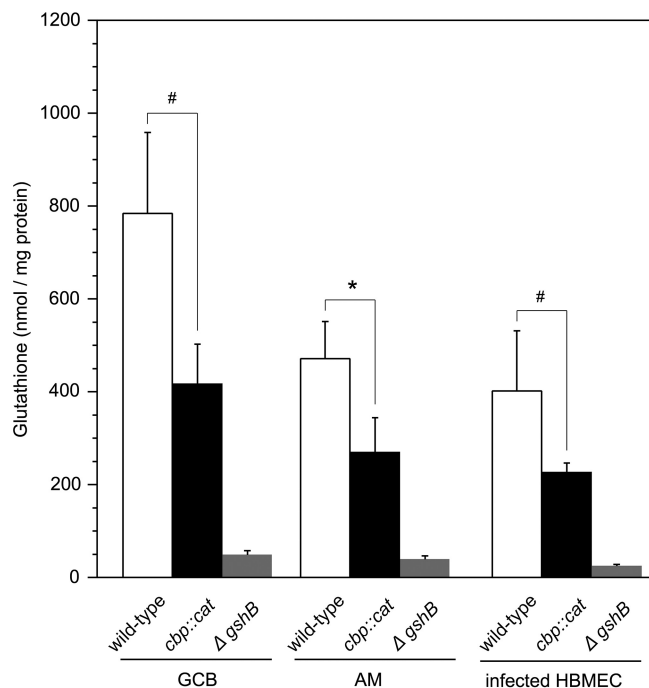


FIG 6 Intracellular glutathione concentrations in *N. meningitidis*. The intracellular glutathione concentration in *N. meningitidis* was measured as described in Materials and Methods. The glutathione concentration in bacteria is expressed as nanomoles of glutathione per mg of bacterial protein. Ranges represent the mean of intracellular glutathione concentrations in *N. meningitidis* in at least four experiments, and error bars represent the standard errors of the means. #, $P < 0.05$; *, $P < 0.003$ (significantly different from the wild-type *cts*⁺ strain).

respiration within the cytoplasm after penetrating the cells (50, 51), was investigated *in vitro* (Fig. 7). The levels of sensitivity to 0.25 and 0.5 mM H₂O₂ did not significantly differ among the wild-type, *cbp* mutant, and $\Delta gshB$ *N. meningitidis* strains (Fig. 7A). However, at 1 mM H₂O₂, the *cbp* mutant was approximately 5-fold more sensitive than the wild-type *N. meningitidis* strain under conditions in which the $\Delta gshB$ mutant was approximately 13-fold more sensitive than the wild-type *N. meningitidis* strain (Fig. 7A). Under these conditions, the *cbp* mutant was approximately 3-fold less sensitive to 1 mM H₂O₂ than the $\Delta gshB$ mutant ($P < 0.001$). These results suggest that a cysteine transport deficiency resulted in *N. meningitidis* being slightly more sensitive to 1 mM H₂O₂. The slight reduction of resistance to 1 mM H₂O₂ was statistically recovered in a *cbp* mutant complemented with HT2080 *cts* genes but not in a *cbp* mutant complemented with a HT2077 *cbp* gene (Fig. S5B). Regarding paraquat, no significant differences were observed with 2 mM paraquat among the wild-type, *cbp* mutant, and $\Delta gshB$ *N. meningitidis* strains (Fig. 7B). At 10 mM paraquat, no significant differences were noted between the wild-type and *cbp* mutant *N. meningitidis* strains, while the $\Delta gshB$ mutant was approximately 7-fold more sensitive than the wild-type and *cbp* mutant *N. meningitidis* strains (Fig. 7B). However, at 50 mM paraquat, the *cbp* mutant was approximately 3-fold more sensitive than the wild-type strain whereas the $\Delta gshB$ mutant was approximately 240-fold more sensitive than the wild-type strain (Fig. 7B). The reduction of resistance to 50 mM paraquat was statistically recovered in a *cbp* mutant complemented with HT2080 *cts* genes but not in a *cbp* mutant complemented with a HT2077 *cbp* gene (Fig. S5C). Collectively, these results with respect to sensitivities to H₂O₂ and paraquat indicated that decreases in glutathione concentrations due to CTS defects did not markedly affect meningococcal resistance to ROS.

Cysteine uptake via the CTS was essential for meningococcal growth in the presence of less than 300 μ M cysteine. We investigated meningococcal growth in liquid media. In the complete medium GCB, the *cbp* mutant grew as efficiently as the

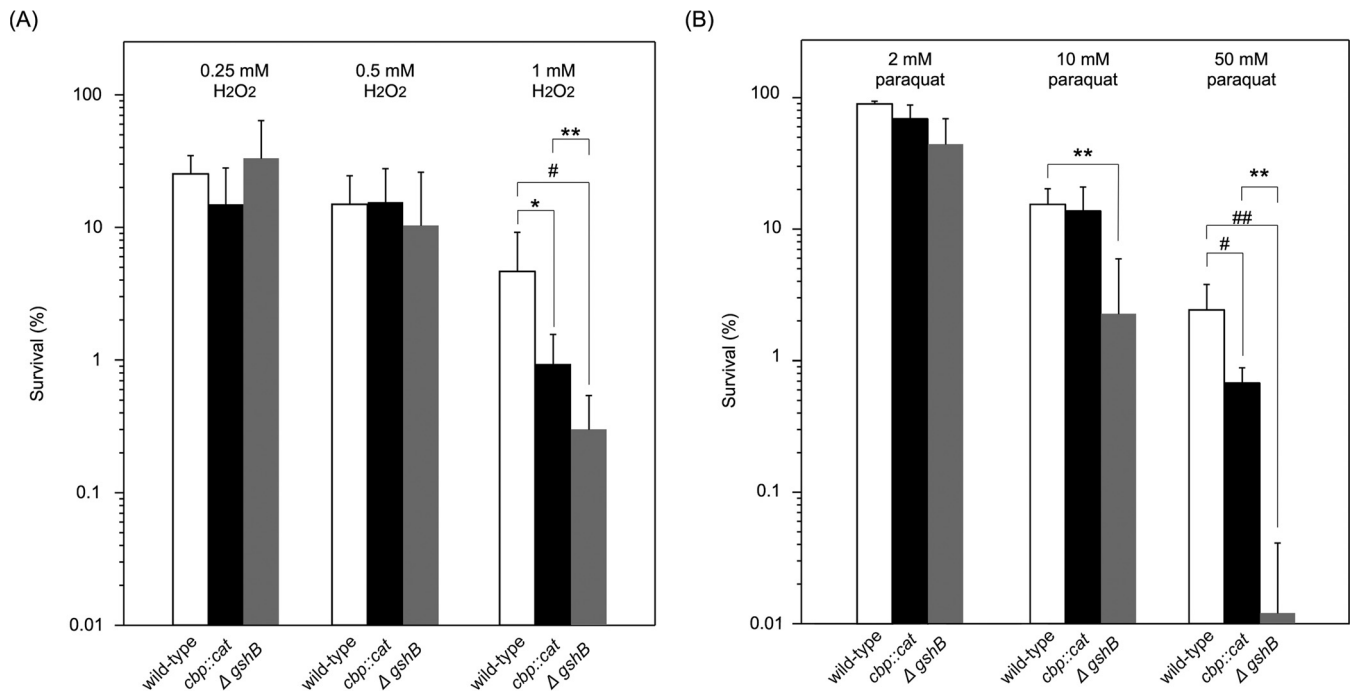


FIG 7 Sensitivity of *N. meningitidis* strains to H₂O₂ and paraquat. Bacteria were incubated at 37°C in GCB with the indicated concentration of H₂O₂ for 15 min (A) and paraquat for 60 min (B). The number of surviving bacteria was counted as CFU by plating onto GC agar plates with appropriate dilutions. Ranges represent the mean percentages of survival in at least five experiments, and error bars show the standard errors of the means. *, $P < 0.05$; #, $P < 0.02$; **, $P < 0.001$; ##, $P < 0.003$ (significantly different from the wild-type *cts*⁺ strain or Δ *gshB::spc* mutant).

wild-type *N. meningitidis* strain (Fig. 8A), indicating that the growth of the *cbp* mutant was not defective in liquid medium. In previous experiments using meningococcal defined medium, Neisseria chemically defined medium (NCDM), developed by Catlin (30), was commonly used for *N. meningitidis* (31, 34). However, under our experimental conditions, most of the *N. meningitidis* strains did not grow in NCDM or grew to an optical density at 600 nm (OD₆₀₀) of ~0.4 from 0.1 at the starting point even though *N. meningitidis* had been precultured on GC agar (data not shown) (38). In order to

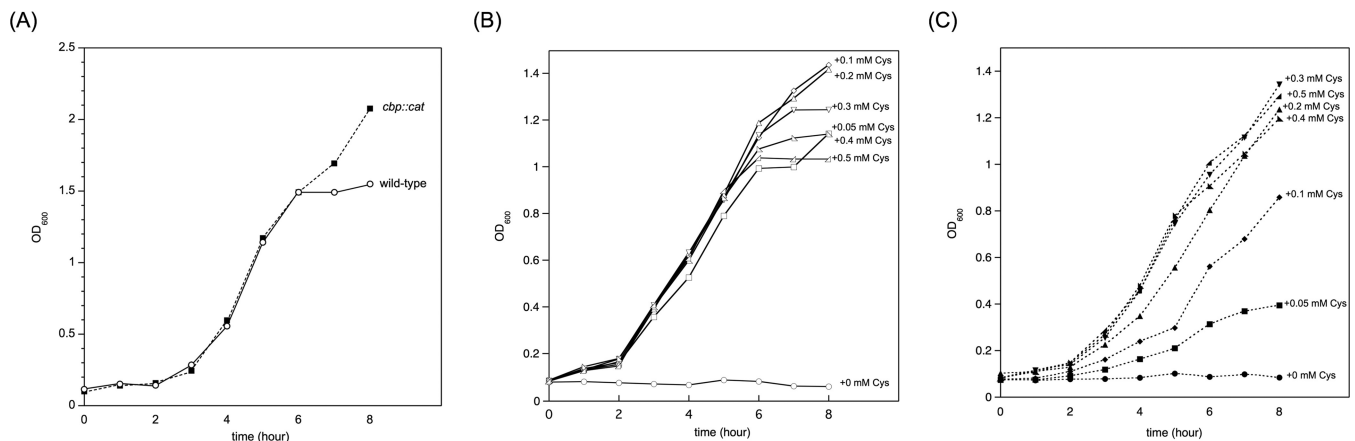


FIG 8 Growth of *N. meningitidis* strains in liquid media. Meningococcal growth was monitored at OD₆₀₀. (A) Meningococcal growth in GCB. Open circles with a solid line and filled circles with a dotted line correspond to wild-type *N. meningitidis* strain NIID84 Δ *cps* and *cbp::cat* mutant HT1959, respectively. Figures show representative data from at least three experiments with similar results. (B and C) Growth of wild-type *N. meningitidis* strain NIID84 Δ *cps* (B) and *cbp::cat* *N. meningitidis* mutant HT1959 (C) in SM devoid of cysteine supplemented with the indicated concentration of cysteine. The following marks indicate the concentration of cysteine supplemented in SM: circle, 0 mM (not supplemented); square, 0.05 mM; diamond, 0.1 mM; triangle, 0.2 mM; inverted triangle, 0.3 mM; right triangle with a right angle on the left, 0.4 mM; right triangle with a right angle on the right, 0.5 mM. Solid lines with open marks and dotted lines with filled marks indicate the growth of wild-type and *cbp::cat* *N. meningitidis* strains, respectively.

overcome this issue, we used our original SM, which was basically the same as NCDM but was supplemented with a one-fourth volume of originally reconstituted MCDB131 devoid of NaCl and cysteine (see Materials and Methods and Table S2 in the supplemental material). Thus, SM did not contain NaCl or cysteine, and these reagents were supplemented if indicated. In SM supplemented with 60 mM NaCl, wild-type *N. meningitidis* strain NIID84 Δcps did not grow when cysteine was not supplemented (Fig. 8B). On the other hand, supplementation of cysteine completely suppressed the growth defect (Fig. 8B), ensuring that meningococcal growth in SM was completely dependent on cysteine. It is important that the supplementation of even 50 μM cysteine was sufficient for meningococcal growth in SM (Fig. 8B). Regarding the growth of the *cbp* mutant, it also did not grow in SM devoid of cysteine (Fig. 8C). The supplementation of increasing concentrations of cysteine gradually suppressed the growth defect in the *cbp* mutant, while at least 300 μM cysteine was required in order to completely suppress the growth defect (Fig. 8C). These results suggest that cysteine uptake via the CTS is crucial for meningococcal growth under conditions of restricted concentrations of cysteine. Furthermore, these results are consistent with the K_m value of meningococcal [^{35}S]cysteine uptake in SM being approximately 114 μM (Fig. 3D). Since the concentration of the intracellular cysteine pool is very limited (approximately 100 μM) (52), these results suggest that the observed marked reduction in bacterial internalization into HBMEC was mostly due to the meningococcal starvation of cysteine in HBMEC (see Discussion).

DISCUSSION

Investigation of the role of metabolism in virulence was recently recognized as a priority equivalent to studying classical virulence factors (24, 26, 53). While cysteine levels in eukaryotes need to be tightly regulated by controlling the degradation of this amino acid (54, 55) and transport of it from the extracellular milieu into the cell and vice versa (56), bacterial cysteine uptake has not yet been elucidated in detail (57–60). *N. meningitidis* cysteine transport and its role in the pathogenesis of meningococcal infections have yet to be clarified. To the best of our knowledge, while all of the experiments in this study were done only by the use of *in vitro* models and with a limited number of meningococcal strains, this is the first study to have suggested a relationship between meningococcal cysteine uptake and the pathogenesis of meningococcal infections.

Although the *N. meningitidis* strains used in the present study were cysteine auxotrophs (Fig. 8), a genome-scale metabolic model suggested that *N. meningitidis* is capable of the *de novo* synthesis of all amino acids, including cysteine (40, 61). However, experimental data revealed contrasting results; some *N. meningitidis* strains, namely, MCS8 (62) and HB-1 (40), grew in minimal defined media, while strain $\alpha 522$ failed to grow (62). Previous studies also demonstrated that cysteine auxotrophs differed among *N. meningitidis* strains (30) and that many *N. meningitidis* strains had cysteine auxotroph characteristics with respect to their growth in the presence of low cysteine concentrations (38–40). While SM used in the present study contained approximately 3 mM inorganic sulfur molecules, which were mainly SO_4^{2-} (see Table S2 in the supplemental material), NIID84 Δcps did not grow in SM if cysteine was supplemented (Fig. 8B). Although further experiments are required to obtain more-comprehensive information, the following may be considered: *N. meningitidis* potentially has a set of genes for *de novo* cysteine synthesis in nature, and no mutation was found in the open reading frame (ORF) of any CTS genes in the genomes of 14 *N. meningitidis* strains recorded in NCBI database (data not shown). However, their products might not be always expressed in all *N. meningitidis* strains because of some negative on the transcription or translation, or enzymes other than CTS enzymes might affect cysteine assimilation but not acquisition for *N. meningitidis*. In fact, the levels of cysteine acquisition ability were different between meningococcal strains and seemed not to be related to the sequence type (see Fig. S6 in the supplemental material) or to the invasive/noninvasive phenotype (63). Regardless of the nature of the cysteine

auxotroph in *N. meningitidis*, the meningococcal ability to uptake cysteine from the surrounding environment would be advantageous for *N. meningitidis* for the following reasons: *N. meningitidis* preferably uses cysteine (cystine) as a sulfur source (41), and *de novo* cysteine synthesis from inorganic sulfur molecules is more laborious and energetically less efficient than cysteine uptake from the surrounding environment because cysteine synthesis requires multiple enzymatic steps (41) with at least one ATP molecule (61). Furthermore, nonessential sulfur is not stored by *N. meningitidis* (36). Therefore, *N. meningitidis* may have to continuously and quickly acquire cysteine for its survival, persistence, and proliferation in humans. Additional experiments are required for more complete understanding of the meningococcal cysteine acquisition.

Three pathogenic bacteria with auxotroph characteristics for cysteine have evolved their own strategies to acquire cysteine in host cells; intracellular *Legionella pneumophila* acquires nutrients that include cysteine by promoting host proteasomal degradation (25) and *Anaplasma phagocytophilum* obtains cysteine by promoting host autophagy (64). *Francisella tularensis* uses glutathione as a cysteine source for intracellular multiplication by γ -glutamyl aminopeptidase (GGT) (52), which is the same strategy used for meningococcal proliferation in CSF (38). However, the results obtained so far have indicated that the intracellular persistence of *N. meningitidis* was not supported by meningococcal GGT because *N. meningitidis* strain HT2022, in which the *ggt* gene was disrupted by the insertion of all three wild-type *cts* genes (Fig. 1), was internalized as efficiently as the wild-type strain (Fig. 2B and C). Regarding pathogenic bacteria that cause meningitis, such as *Haemophilus influenzae* and *Streptococcus pneumoniae*, while limited information is currently available on the role of cysteine in the pathogenesis of meningitis, the cysteine synthesis gene in *S. pneumoniae* was shown to be transcriptionally upregulated in the presence of low cysteine concentrations (65). While meningococcal glutamate uptake was also regulated by Na concentration (31), the meningococcal cysteine uptake activity was not regulated by Na (Fig. S3C), leading to the speculation that the activity might be not altered by environmental conditions.

Compared to the large reduction in the intracellular survival rate (Fig. 5B), [³⁵S]Cys uptake in the *cbp* mutant decreased to only approximately 40% of the level seen in the wild-type strain (Fig. 3A). The discrepancy might have been due to the experimental conditions used for analysis of [³⁵S]Cys uptake in this study; the [³⁵S]Cys obtained in our laboratory tended to bind nonspecifically to meningococci as well as to any chemical filter (e.g., polyvinylidene difluoride [PVDF] and glass) even though they were washed with excess amounts of phosphate-buffered saline (PBS) containing 2% saponin (data not shown). Since no other cysteine uptake system was found in the meningococcal genome database uploaded (data not shown), the CTS would seem to be unique with respect to meningococcal cysteine acquisition, and it was also shown that the [³⁵S]Cys uptake in the *cbp* mutant could not be observed even for 5 min of incubation with a high concentration of [³⁵S]Cys in buffer A instead of SM (Fig. S3A). Thus, it would also seem to be possible that the [³⁵S]Cys uptake examined in SM in this study was overestimated against the true function of cysteine uptake via the CTS in *N. meningitidis* and that methods used to address the problems regarding [³⁵S]Cys uptake could be further improved.

The *cbp* mutant grew normally (similarly to the wild-type strain) in GCB (Fig. 8A), eliminating the possibility that a mutation in meningococcal CTS itself affected essential *N. meningitidis* growth. It should be noted that the *cbp* mutant grew better than the wild-type strain in GCB at the stationary phase (Fig. 8A), which might be related to the negative effect of cysteine for bacterial growth (discussed below). On the other hand, under cysteine-limited conditions, while the supplementation of at least 50 μ M cysteine was sufficient to suppress the growth defect in cysteine-free SM in the wild-type strain (Fig. 8B), supplementation of more than 300 μ M cysteine was required for the complete suppression of growth of the *cbp* mutant (Fig. 8C). These results suggest that meningococcal cysteine uptake mediated via the CTS plays an essential role in *N. meningitidis* growth under conditions of low cysteine concentrations. On the basis of

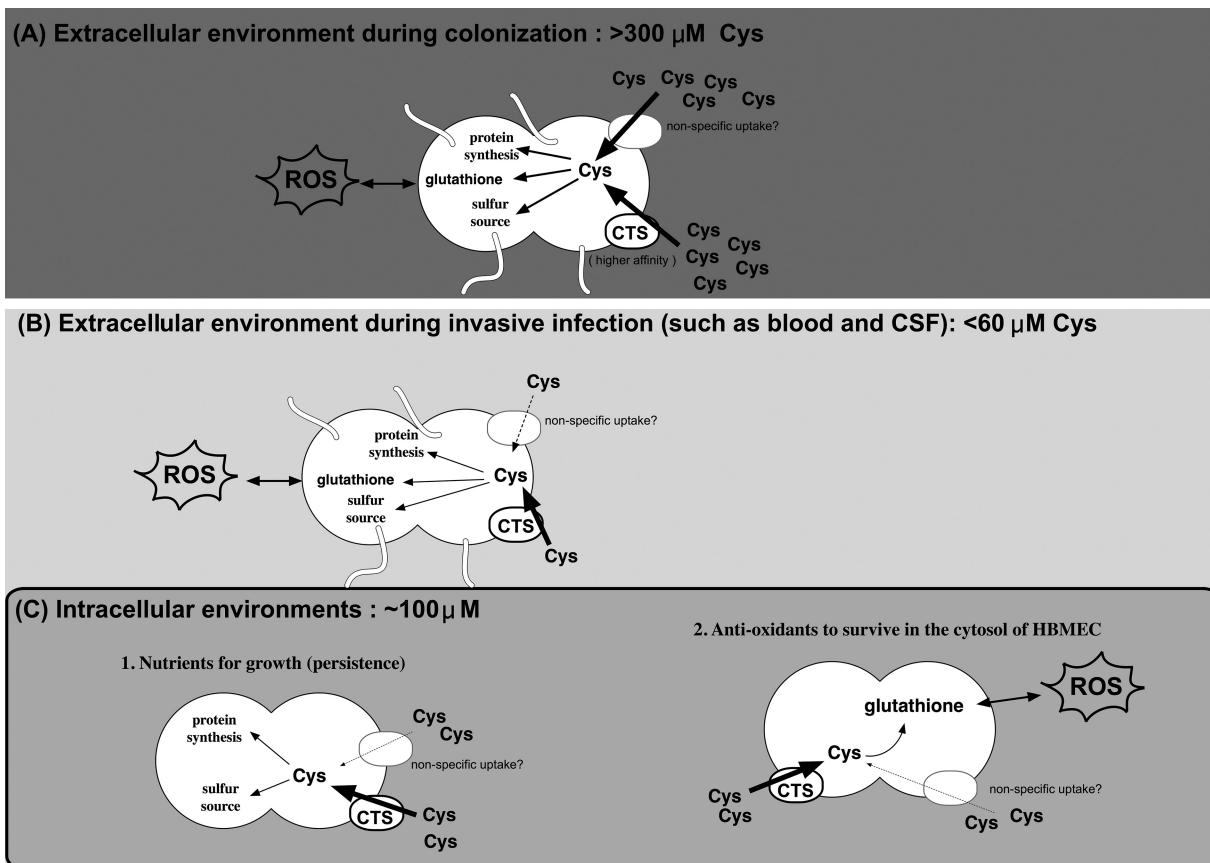


FIG 9 Schematic representation of meningococcal infections in humans. Since *cbp* *N. meningitidis* grew in cysteine-rich medium (GCB) (Fig. 8A), *N. meningitidis* may have two cysteine transport systems: a CTS that functions under low-cysteine conditions (higher affinity for cysteine) and an unidentified cysteine transporter that may function only under cysteine-rich conditions (lower affinity for cysteine). While this study showed only the intracellular functions of cysteine uptake via the CTS in *N. meningitidis* (C), this physiological function may be extensively applied to all human milieus for meningococcal infections in humans on the basis of the following concept. During the course of meningococcal invasion, until the point at which *N. meningitidis* reaches the human cells, *N. meningitidis* encounters at least 3 types of environments in humans: (A) the environment outside the human (e.g., nasopharynx), (B) the environment inside humans but not the intracellular milieu (e.g., blood and CSF), and (C) the intracellular milieu (in epithelial and endothelial cells). Cysteine is not limited in the environment represented in panel A because sufficient cysteine is supplied from the digestion of food. However, cysteine availability is very limited inside human environments (B and C) due to nutrient immunity with respect to cysteine. Cysteine concentrations in extracellular environments in humans (B) in blood (~50 μM) and CSF (~1 μM) are lower than in the intracellular milieu (A). The limitation of cysteine availability is also found in the intracellular environment, in which the concentration of cysteine is estimated to be approximately 100 μM. Thus, *N. meningitidis* has to “dive” into humans to cause IMD, in which context the milieu cysteine availability is always limited by the human nutrient immunity.

the cysteine concentrations seen in humans, meningococcal cysteine uptake via the CTS is advantageous for *N. meningitidis* (Fig. 9); the concentration of cysteine in the human nasopharynx remains unclear, but the nasopharynx is considered to be one of the nutritionally richest niches in humans because cysteine is supplied from the digestion of food. Alternatively, cysteine may be supplied from nasopharyngeal commensal bacteria. On the other hand, when *N. meningitidis* enters and passes through human epithelial and endothelial cells by endocytosis, the intracellular cysteine concentration is very low at approximately 100 μM (52). When the organism enters the bloodstream, the concentration of cysteine in human blood plasma is only approximately 30 to 60 μM (65, 66). During inflammation with sepsis, the cysteine concentration is significantly decreased (67, 68). *N. meningitidis* attaches again to endothelial cells comprising the BBB, passes through cells or loosens tight junctions (47), and enters the CSF. The concentration of cysteine in the CSF is very limited at less than 1 μM (38). Thus, cysteine concentrations are very low in humans (69) because mammals synthesize cysteine from methionine and serine, and cysteine may also be supplied from glutathione (70), which is an abundant and ubiquitous molecule in all organs and cell types

(48). The limitation of the availability of “free” cysteine in humans may be regarded as a type of nutrient immunity. Therefore, the meningococcal cysteine acquisition via the CTS may play an important role as a “nutrient virulence factor” for *N. meningitidis* infections in humans with nutrient immunity for cysteine (Fig. 9).

In the present study, we used unencapsulated *N. meningitidis* strains for efficient internalization by eliminating the multiple effects of the capsule on meningococcal infections in humans. As discussed in our previous study (33), the meningococcal capsule may affect the intracellular survival ability (Fig. 5). However, since the majority of internalized bacteria are considered to remain unencapsulated until a phase variation occurs (8, 71), the intracellular survival of the unencapsulated state may also be important in the *N. meningitidis* infectious cycle. Furthermore, since the capsule expression does not hinder the import of amino acid into *N. meningitidis* (34), cysteine uptake in *N. meningitidis* is physiologically advantageous for the infection of humans regardless of the capsule expression state.

While cysteine is an important amino acid because it contains sulfur, which plays a vital role in the catalytic sites of many enzymes and participates in ion and redox metabolism (72), excessive amounts of cysteine are also harmful for many bacteria (73). For example, *Escherichia coli*, which is a prototroph for cysteine, did not synthesize excess amounts of (74) or store (75) cysteine by feedback pathways. This may also be the case for *N. meningitidis* because the supplementation of a higher concentration of cysteine appeared to inhibit meningococcal growth in SM at the late logarithmic phase (Fig. 8B) and the addition of 1 mM cysteine also appeared to inhibit meningococcal growth in SM (data not shown). Since cysteine auxotrophic organisms have to control intracellular cysteine concentrations at its uptake only, it seems reasonable to hypothesize that slow cysteine uptake via the CTS in *N. meningitidis* is among its advantageous biological functions.

The exploitation of host nutrients by pathogens is a major factor in host-pathogen interactions and is one of the fundamental aspects of infectious diseases; however, our knowledge of microbial metabolism in hosts is limited. Further studies on the mechanisms underlying microbial (including meningococcal) “nutritional virulence” and metabolism *in vivo* will provide a more comprehensive understanding of the central aspect of infectious diseases and result in the development of treatments and prevention strategies, such as the development of inhibitors for folate metabolism in pathogenic bacteria (76) or for iron acquisition using antibodies against *N. meningitidis* transferrin-binding proteins (77).

MATERIALS AND METHODS

Bacterial growth conditions. *N. meningitidis* strains (stored at -80°C) were routinely grown on GC agar plates at 37°C in a 5% CO_2 atmosphere (78). Brain heart infusion (Becton, Dickinson, USA) agar containing 3% defibrinated horse blood (Nihon Biotest, Japan) was used in the selection of kanamycin-resistant *N. meningitidis* strains (63). *E. coli* was grown on L plates or in L broth liquid cultures at 37°C . When required, antibiotics were added at the following concentrations: kanamycin at $150\ \mu\text{g/ml}$, chloramphenicol at $5\ \mu\text{g/ml}$, and spectinomycin at $75\ \mu\text{g/ml}$ for *N. meningitidis* and kanamycin at $50\ \mu\text{g/ml}$ and ampicillin at $50\ \mu\text{g/ml}$ for *E. coli*. The *N. meningitidis* strains used in the present study are listed in Table 1.

GC broth (GCB) contained the following (per liter); proteose peptone, 15 g; NaCl, 5 g; soluble starch, 0.5 g; K_2HPO_4 , 1 g; KH_2PO_4 , 4 g; IsoVitaleX enrichment (Difco), 10 ml; 1 M NaHCO_3 , 5 ml; 1 M MgCl_2 , 10 ml.

SM in the present study basically consisted of NCDM (30), except that NaCl and cysteine were omitted (details were shown in Table S2 in the supplemental material). NaCl and cysteine were added when required. Additionally, due to another nutrient requirement(s), most meningococcal strains in our laboratory did not grow in NCDM (data not shown). In order to overcome this issue, MCDB131 (Thermo Fisher) lacking cysteine and NaCl, which was specifically manufactured by Cell Science & Technology Inst. Inc. (Japan), was added to a one-fourth volume in a final volume of 10 ml NCDM (details of the contents are shown in Table S2).

Construction of meningococcal mutants. *N. meningitidis* strains that did not produce a capsule were constructed by transformation with the purified chromosomal DNA of HT1034 ($\Delta\text{siaB}\ \Delta\text{siaD}::\text{kan}$) (63), and kanamycin-resistant clones were selected (Table 1). The transformation of *N. meningitidis* strains was performed as described previously (78).

In order to construct the *N. meningitidis* *cbp* insertion mutant, a 0.8-kb DNA fragment from *N. meningitidis* H44/76 chromosomal DNA containing the *cbp* gene was amplified with primers *cbp*-1 and *cbp*-2 (Table S1) by the use of PrimeSTAR Max DNA polymerase (TaKaRa Bio, Japan) and was cloned into

TABLE 1 Strains used in this study

Strain	Genotype	Parent strain	Source
<i>N. meningitidis</i> strains			
NIID84	Wild-type strain (ST-33, serogroup B)		This study
NIID512	Wild-type strain (ST-687, serogroup B)		This study
NIID521	Wild-type strain (ST-8959, serogroup B)		This study
NIID84 Δ <i>cps</i>	Δ <i>siaB</i> Δ <i>siaD::kan</i>	NIID84	This study
HT1959	Δ <i>siaB</i> Δ <i>siaD::kan</i> <i>cbp::cat</i>	NIID84 Δ <i>cps</i>	This study
HT2077	Δ <i>siaB</i> Δ <i>siaD::kan</i> <i>cbp::cat</i> <i>ggt::Ptac</i> <i>cbp</i> ⁺ <i>spc</i>	HT1959	This study
HT2080	Δ <i>siaB</i> Δ <i>siaD::kan</i> <i>cbp::cat</i> <i>ggt::cbp</i> ⁺ <i>ctp</i> ⁺ <i>cab</i> ⁺ <i>spc</i>	HT1959	This study
NIID512 <i>cps</i> -	Δ <i>siaB</i> Δ <i>siaD::kan</i>	NIID512	This study
HT2056	Δ <i>siaB</i> Δ <i>siaD::kan</i> <i>cbp::cat</i>	NIID512 Δ <i>cps</i>	This study
HT2078	Δ <i>siaB</i> Δ <i>siaD::kan</i> <i>cbp::cat</i> <i>ggt::Ptac</i> <i>cbp</i> ⁺ <i>spc</i>	HT2056	This study
HT2081	Δ <i>siaB</i> Δ <i>siaD::kan</i> <i>cbp::cat</i> <i>ggt::cbp</i> ⁺ <i>ctp</i> ⁺ <i>cab</i> ⁺ <i>spc</i>	HT2056	This study
NIID521 Δ <i>cps</i>	Δ <i>siaB</i> Δ <i>siaD::kan</i>	NIID521	This study
HT2063	Δ <i>siaB</i> Δ <i>siaD::kan</i> <i>cbp::cat</i>	NIID521 Δ <i>cps</i>	This study
HT2079	Δ <i>siaB</i> Δ <i>siaD::kan</i> <i>cbp::cat</i> <i>ggt::Ptac</i> <i>cbp</i> ⁺ <i>spc</i>	HT2063	This study
HT2082	Δ <i>siaB</i> Δ <i>siaD::kan</i> <i>cbp::cat</i> <i>ggt::cbp</i> ⁺ <i>ctp</i> ⁺ <i>cab</i> ⁺ <i>spc</i>	HT2063	This study
HT2120	Δ <i>siaB</i> Δ <i>siaD::kan</i> Δ <i>gshB::spc</i>	NIID84 Δ <i>cps</i>	This study
<i>Escherichia coli</i> strains			
JM109	<i>endA1 gyrA96 hsdR17(r_K⁻ m_K⁺) mcrB⁺ recA1 relA1 supE44 thi-1 Δ(<i>lac-proAB</i>) F[<i>traD36, proAB, lacI^qZ</i>ΔM15]</i>		Nippon Gene
BL21(DE3)	<i>fhuA2 [lon] ompT gal (λ DE3) [dcm] Δhds λ DE3 = λ sBamHlo ΔEcoRI-B int::(<i>lacI::PlacUV5::T7 gene1</i>) i21 Δnin5</i>		NEB

the SmaI site of the pMW119 vector (Nippon Gene, Japan) (4.2 kb) to construct pHT1319 (5 kb). The 5-kb DNA region of pHT1319 was amplified with primers *cbp*-3 and *cbp*-4, which separated the *cbp* structural gene into 400 and 425 bp, respectively, by the use of PrimeSTAR Max DNA polymerase and was ligated with a chloramphenicol resistance gene (*cat*) to construct pHT1328. A 1.8-kb DNA fragment containing the *cbp* structural gene insertionally disrupted with the *cat* gene was amplified with primers *cbp*-1 and *cbp*-2 from pHT1328 and transformed into *N. meningitidis* strains, and chloramphenicol-resistant clones were selected, resulting in *cbp* insertional mutants (Table 1).

A *cbp* mutant complemented with the *cbp*⁺ gene at the *ggt* allele was constructed as follows. A 0.8-kb *cbp* gene was amplified with primers pTTQ-1-*cbp*-5 and M13-47-*cbp*-6. A 4.3-kb DNA fragment was also amplified from pTTQ18 (79) with primers pTTQ-2(PO+RBS) and M13-47 reverse (Table S1). These two DNA fragments were connected by the use of SLiCE (80). The resultant plasmid was named pHT1381. In order to insert a spectinomycin resistance gene (*spc*) downstream of the *cbp* gene, a 5.1-kb DNA fragment was amplified from pHT1381 with primers pTTQ-5 and pTTQ-6 (Table S1). A 1-kb *spc* gene was also amplified from pHT154 (81) with primers pTTQ-5'(15mer)-M13-RV-Long and pTTQ-6'(15mer)-M13-47-Long. These two DNA fragments were connected by the use of SLiCE, resulting in a plasmid that was named pHT1386. A 3-kb DNA fragment containing the *Ptac*, *cbp*, and *spc* genes was amplified from pHT1386 with primers *ggt*-5'(15mer)-*ptac*-13 and *ggt*-3'(15mer)-*ptac*-14 and was inserted into a BstXI site (at the middle of the *ggt* coding region) of pHT624, in which the *ggt* gene harbored by pHT195 (81) was subcloned into pMW119, resulting in pHT1387. A 4.5-kb DNA fragment containing the *ggt::Ptac* *cbp* *spc* genes was amplified with primers *ggt*-1 and *ggt*-2 (82) and transformed into the *N. meningitidis* *cbp::cat* mutants, and spectinomycin-resistant (*Spc*^r) clones were selected, resulting in *cbp* insertional mutants ectopically complemented with the *cbp* gene expressed from the *tac* promoter at the *ggt* allele (Table 1).

A *cbp* mutant complemented with all three *cts* genes (*cbp*, *ctp*, and *cab*) at the *ggt* allele was constructed as follows: a 3.3-kb DNA fragment containing *cts* genes was amplified from NIID84 chromosomal DNA with primers *cts* operon-1 and *cts* operon-2 and cloned into the SmaI site of pMW119, resulting in pHT1391. In order to insert the *spc* gene downstream of the *cab* gene, a 7.6-kb DNA fragment was amplified from pHT1391 with primers M13-47'(15mer)-pMW(MCS)-down-1 and M13-RV'(15mer)-pMW(MCS)-down-2 (Table S1). A 1-kb *spc* gene was amplified from pHT154 with the universal primers M13-RV and M13-47, and these two DNA fragments were connected by the use of SLiCE, resulting in pHT1393. A 4.3-kb DNA fragment containing *cts* genes and the *spc* gene was amplified from pHT1393 with primers *ggt*-5'(15mer)-pMW119-F and *ggt*-3'(15mer)-pMW119-R (Table S1) and cloned into a BstXI site of pHT624 by the use of SLiCE, resulting in a plasmid that was named pHT1395. A 6.3-kb DNA fragment containing the *ggt::cbp* *ctp* *cab* *spc* genes was amplified from pHT1395 with primers *ggt*-1 and *ggt*-2 and transformed into the *N. meningitidis* *cbp::cat* mutants, and *Spc*^r clones were selected, resulting in *cbp* insertional mutants ectopically complemented with the *cts* genes expressed from their own promoter at the *ggt* allele (Table 1).

A *N. meningitidis* mutant deleted of the *gshB* gene was constructed by transformation with a 2-kb DNA fragment containing the Δ *gshB::spc* construct amplified from pHT1058 (33), and *Spc*^r clones were selected and named HT2120 (Table 1).

Production of anti-Cbp protein rabbit antiserum. A 768-bp DNA fragment devoid of the N-terminal putative hydrophobic domain of Cbp (18 amino acids) was amplified with a set of primers

(cbp-1(BamHI) and cbp-2(HindIII)) from NIID84 chromosomal DNA by Prime STAR Max polymerase. The DNA fragment was digested with BamHI and HindIII and was cloned into the same cutting sites of expression vector pET24a (Invitrogen), resulting in pHT1376. The plasmid pHT1376 was transformed into *E. coli* strain BL21(DE3) (NEB), and the transformant was cultured in 150 ml MagicMedia (Invitrogen) at 30°C overnight with shaking. The subsequent purification of a recombinant protein and generation of polyclonal rabbit serum to the putative hydrophilic domain of the Cbp protein were performed as described previously (81).

RT-PCR. Bacteria grown on GC agar plates were suspended in 20 ml of GC to an OD₆₀₀ of 0.1 and continuously cultured to mid-log phase (OD₆₀₀ of ~0.6) at 37°C with shaking. The total RNA was isolated from the harvested bacteria using a FastGene RNA Premium kit (Nihon Genetics, Japan). RT-PCR was performed using a SuperScript III One-Step RT-PCR system with Platinum *Taq* DNA polymerase (Invitrogen) and approximately 0.1 µg of total RNA according to the manufacturer's instructions. Reverse transcriptase reactions (50°C for 30 min) were omitted (-RT in Fig. S2 in the supplemental material) to confirm that the amplicon was derived from RNA. The products were visualized by electrophoresis in a 2% agarose gel followed by ethidium bromide staining.

Tissue culture. HBMEC were cultivated as described previously (63). In each experiment, HBMEC were seeded in a culture flask or dish or on a cover glass and were used within 2 days of reaching confluence.

Assessment of host cell-associated and internalized bacteria. HBMEC were cultivated on gelatin-coated 96-well tissue culture plates (Iwaki, Japan) at 37°C for 2 days in a 5% CO₂ atmosphere to a concentration of 1×10^4 cells/well. Two hours prior to bacterial infection, the culture medium was replaced with assay medium (AM), which was MCDB131 (Invitrogen) supplemented with 10% fetal bovine serum (FBS), 90 µg ml⁻¹ heparin, and 3 mM glutamine. The bacterial suspension was prepared in AM at an OD₆₀₀ of 0.05, which corresponded to approximately 5×10^6 CFU/100 µl. The multiplicity of infection (MOI) was 500, a condition previously used in other studies (45, 83), to examine efficient *N. meningitidis* internalization (33, 42). A 100-µl portion of the bacterial suspension was inoculated onto host cell monolayers in duplicate for each assay, and the reaction mixtures were incubated at 37°C for 4 h in a 5% CO₂ atmosphere. In order to evaluate bacterial adherence, the monolayers were washed with prewarmed AM four times to remove nonadherent bacteria. Adherent bacteria were released by the addition of phosphate-buffered saline (PBS) containing 2% saponin, and CFU levels were assessed on GC agar plates with appropriate dilutions to count cell-adherent bacteria. In order to evaluate internalized bacteria, AM containing 150 µg ml⁻¹ of gentamicin was added, and cultures were incubated for 1 h in order to kill all extracellular bacteria. Almost all (>99.999%) of up to 5×10^7 extracellular meningococci were killed under these experimental conditions (data not shown). The amounts of internalized bacteria that were not killed by the gentamicin treatment were assessed by the addition of PBS containing 2% saponin and by plating on GC agar after appropriate dilutions were made to count bacterial numbers as CFU levels. Results are expressed as means ± standard deviations (SD), and bacterial numbers were statistically compared using the two-tailed Student's *t* test.

Western blotting. *N. meningitidis*, grown on GC agar plates, was suspended in PBS. Bacteria were harvested at an OD₆₀₀ of 20 and resuspended in 1 ml 1× SDS buffer and boiled for 10 min. SDS-PAGE and Western blotting were performed as described previously (38).

Bacterial L-cysteine uptake assay. The L-cysteine transport assay was performed as follows. *N. meningitidis* strains grown overnight on GC agar plates at 37°C in 5% CO₂ were suspended in 2 ml buffer A (50 mM potassium buffer [pH 7.0] and 0.5 mM MgCl₂) (31, 32) and harvested by centrifugation at $10,000 \times g$ at 4°C for 2 min. The bacterial pellet was resuspended in 2 ml buffer A and centrifuged again. These procedures were repeated 3 times to wash bacteria. The resultant pellets were suspended in 1 ml buffer A to adjust the bacterial concentration at an OD₆₀₀ of 10. Ten microliters of 300 µM L-[³⁵S]cysteine (America Radiolabeled Chemicals) (specific activity, 1,075 Ci/mmol) was mixed with 10 µl of a 3-fold-higher concentration of SM containing 180 mM NaCl under standard conditions. A 3-fold concentration of L-[³⁵S]cysteine was added to the reaction mixture when substrate dependency for CTS was examined (Fig. 3C; see also Fig. S3A). The mixture was prewarmed at 37°C for 5 min. Assays were initiated by the addition of 10 µl of the bacterial suspension and was incubated at 37°C for 5 min. Further incubations were performed to optimize the incubation time (Fig. 3B; see also Fig. S3B). The reaction was terminated by the removal of substrates by subsequent maximal centrifugation at 4°C for 1 min. The resultant pellet (bacteria) was washed 3 times with 0.5 ml PBS containing 2% saponin. The resultant pellet was resuspended in 50 µl buffer A. Radioactivity was assessed by scintillation counting in an 8-ml vial containing 5 ml Filtron-X (National Diagnostics, USA). The nonspecific binding of L-[³⁵S]cysteine to bacteria was assessed in control bacterial samples that were inactivated at 70°C for 30 min, and the value obtained was subtracted from all experimental values. Protein concentrations were measured using a bicinchoninic acid (BCA) protein assay kit (Thermo), with bovine serum albumin (BSA) used as a standard. L-Cysteine transport values were expressed as means ± SD representing nanomoles of substrate transported per minute per milligram of bacterial protein.

Observations of meningococci and ezrin accumulation by immunofluorescence staining. HBMEC monolayers, grown on a cover glass at 37°C in a 5% CO₂ atmosphere for 2 days, were infected with *N. meningitidis* in AM at an MOI of 500 for 4 h. The infected HBMEC monolayers were washed four times with 500 µl prewarmed AM, fixed with 4% paraformaldehyde-PBS for 15 min, permeabilized with 0.2% Triton X-100-PBS, and blocked with 2% BSA-PBS for 30 min. The resultant monolayers were incubated with the anti-ezrin monoclonal 3C12 antibody (Santa Cruz, USA) and diluted 100-fold for 45 min and then with the Alexa Fluor 488-conjugated F(ab') fragment of anti-mouse IgG (Invitrogen) and then diluted 200-fold for 45 min under moist and dark conditions. Glass coverslips were mounted on a glass slide with

ProLong Gold antifade reagent (Invitrogen). Infected HBMEC and the attached meningococci were observed using a BX51 microscope with a 100× oil immersion objective.

Monitoring meningococcal survival in HBMEC. A meningococcal intracellular survival assay in HBMEC was performed as follows. Confluent HBMEC monolayers seeded on gelatin-coated 24-well tissue culture plates (Iwaki) were infected with meningococci at an MOI of 5,000 for 2 h in order to obtain the maximal amount of internalized bacteria (32). A high dosage of meningococci did not exert any cytotoxic effect on HBMEC (data not shown). Monolayers were washed with AM four times and then incubated with AM containing 150 $\mu\text{g ml}^{-1}$ gentamicin for 1 h in order to kill extracellular bacteria. Gentamicin-containing AM was replaced with AM, and the reaction mixtures were incubated further at 37°C in 5% CO₂ to monitor the number of bacteria in HBMEC. This time point was defined as time zero. Intracellular bacteria were measured at time zero and after 1, 2, 3, and 4 h, and bacterial numbers were counted as CFU by plating on GC agar plates after appropriate dilutions. Survival percentages were calculated by the following formula: $100 \times (\text{CFU at the indicated hour(s)})/(\text{CFU at time zero})$. The results were expressed as means \pm SD.

Measurement of glutathione concentrations in bacteria only or bacteria that infected HBMEC. *N. meningitidis* strains grown on GC agar plates at 37°C overnight in 5% CO₂ were suspended in 15 ml AM or GCB in order to adjust the bacterial concentration to an OD₆₀₀ of 0.15/ml and were then incubated at 37°C for 4 h in 5% CO₂, or bacteria were used to infect HBMEC seeded on a 150-mm-diameter dish at an MOI of 500 for 4 h. Bacterial samples were prepared as described previously (33). In brief, harvested bacteria were suspended in 1 ml H₂O and were centrifuged at 10,000 $\times g$ at 4°C for 2 min. This procedure was repeated 3 times. The resultant pellets were suspended in 100 μl of 0.5% sulfosalicylic acid, and bacteria were lysed using three freeze/thaw cycles, briefly sonicated, and centrifuged again at 14,000 $\times g$ at 4°C for 10 min. The glutathione concentration in the supernatant was measured with a total glutathione quantification kit (Dojindo, Japan). Protein concentrations were measured with a BCA protein assay kit. Glutathione concentrations in bacteria were expressed as means \pm SD of nanomoles of glutathione per milligram of bacterial protein.

Assay of sensitivity to H₂O₂ and paraquat *in vitro*. *N. meningitidis* strains grown on GC agar plates at 37°C overnight in 5% CO₂ were suspended in 1.5 ml GCB, and the bacterial suspension was prepared in 1 ml GCB at an OD₆₀₀ of 0.01, which corresponded to 1×10^7 bacteria/ml. The indicated concentration of H₂O₂ (0.25, 0.5, or 1 mM) or paraquat (2, 5, or 50 mM), which represents the conditions normally applied to *in vitro* neisserial analyses (51, 84–87), was added to 1 ml of the bacterial suspension and incubated at 37°C for 15 min (for H₂O₂) or for 60 min (for paraquat) with gentle shaking. Surviving bacteria were counted as CFU by plating on GC agar plates after appropriate dilutions. The CFU of bacteria not treated with H₂O₂ or paraquat at time zero was defined as 100%, and the survival rate was calculated using the following formula: $100 \times (\text{CFU treated with H}_2\text{O}_2 \text{ or paraquat})/(\text{CFU not treated with H}_2\text{O}_2 \text{ or paraquat})$.

Monitoring of *N. meningitidis* growth in liquid media. *N. meningitidis* strains grown on GC agar plates at 37°C overnight in 5% CO₂ were suspended in 10 ml buffer A and centrifuged at 7,000 $\times g$ for 2 min. The bacterial pellet was resuspended in 10 ml buffer A and centrifuged again. This procedure was repeated 3 times. The resultant pellets were suspended in 5 ml buffer A. Bacterial suspensions were prepared at an OD₆₀₀ of 0.1 in 10 ml GCB or SM supplemented with the indicated concentration of cysteine. Since the cysteine solution was made from cysteine HCl salt, the same amount and concentration of NaOH solution were added for neutralization. Bacteria were cultivated at 37°C with shaking at a rate of 160 rpm/min. Meningococcal growth was monitored as OD₆₀₀ by the use of a SmartSpec Plus spectrophotometer (Bio-Rad).

Statistical analyses. Results are expressed as means \pm SD. Results of determinations of adhered and internalized bacterial numbers, ratios of internalized/adhered bacteria, glutathione measurements, L-cysteine uptake measurements, and meningococcal survival measurements in HBMEC were compared using the two-tailed Student's *t* test, and *P* values of <0.05 were considered to be significant.

SUPPLEMENTAL MATERIAL

Supplemental material for this article may be found at <https://doi.org/10.1128/mBio.02332-18>.

FIG S1, TIF file, 0.4 MB.

FIG S2, TIF file, 1.9 MB.

FIG S3, TIF file, 0.7 MB.

FIG S4, TIF file, 0.4 MB.

FIG S5, TIF file, 0.7 MB.

FIG S6, TIF file, 0.4 MB.

TABLE S1, DOCX file, 0.1 MB.

TABLE S2, DOCX file, 0.1 MB.

ACKNOWLEDGMENTS

This work was supported by JSPS KAKENHI and AMED (JSPS KAKENHI grant number 15K08485 [H.T.]; AMED grant number 18fk0108071j0101 [H.T.]).

REFERENCES

- Takahashi H, Haga M, Sunagawa T, Saitoh T, Kitahara T, Matsumoto S, Ohnishi M. 2016. Meningococcal carriage rates in healthy individuals in Japan determined using loop-mediated isothermal amplification and oral throat wash specimens. *J Infect Chemother* 22:501–504. <https://doi.org/10.1016/j.jiac.2015.12.016>.
- Chang Q, Tzeng YL, Stephens DS. 2012. Meningococcal disease: changes in epidemiology and prevention. *Clin Epidemiol* 4:237–245.
- Brouwer MC, Read RC, van de Beek D. 2010. Host genetics and outcome in meningococcal disease: a systematic review and meta-analysis. *Lancet Infect Dis* 10:262–274. [https://doi.org/10.1016/S1473-3099\(10\)70045-1](https://doi.org/10.1016/S1473-3099(10)70045-1).
- Murray RL, Britton J, Leonardi-Bee J. 2012. Second hand smoke exposure and the risk of invasive meningococcal disease in children: systematic review and meta-analysis. *BMC Public Health* 12:1062. <https://doi.org/10.1186/1471-2458-12-1062>.
- Rashid H, Booy R. 2012. Passive smoking, invasive meningococcal disease and preventive measures: a commentary. *BMC Med* 10:160. <https://doi.org/10.1186/1741-7015-10-160>.
- Codjoe SN, Nabie VA. 2014. Climate change and cerebrospinal meningitis in the Ghanaian meningitis belt. *Int J Environ Res Public Health* 11:6923–6939. <https://doi.org/10.3390/ijerph110706923>.
- Simonis A, Schubert-Unkmeir A. 2016. Interactions of meningococcal virulence factors with endothelial cells at the human blood-cerebrospinal fluid barrier and their role in pathogenicity. *FEBS Lett* 590:3854–3867. <https://doi.org/10.1002/1873-3468.12344>.
- Virji M. 2009. Pathogenic neisseriae: surface modulation, pathogenesis and infection control. *Nat Rev Microbiol* 7:274–286. <https://doi.org/10.1038/nrmicro2097>.
- Pizza M, Rappuoli R. 2015. *Neisseria meningitidis*: pathogenesis and immunity. *Curr Opin Microbiol* 23:68–72. <https://doi.org/10.1016/j.mib.2014.11.006>.
- Schubert-Unkmeir A. 3 March 2017. Molecular mechanisms involved in the interaction of *Neisseria meningitidis* with cells of the human blood-cerebrospinal fluid barrier. *Pathog Dis* <https://doi.org/10.1093/femspd/ftx023>.
- Serruto D, Adu-Bobie J, Scarselli M, Veggi D, Pizza M, Rappuoli R, Aricò B. 2003. *Neisseria meningitidis* App, a new adhesin with autocatalytic serine protease activity. *Mol Microbiol* 48:323–334. <https://doi.org/10.1046/j.1365-2958.2003.03420.x>.
- Capecchi B, Adu-Bobie J, Di Marcello F, Ciocchi L, Masignani V, Taddei A, Rappuoli R, Pizza M, Aricò B. 2004. *Neisseria meningitidis* NadA is a new invasin which promotes bacterial adhesion to and penetration into human epithelial cells. *Mol Microbiol* 55:687–698. <https://doi.org/10.1111/j.1365-2958.2004.04423.x>.
- van Ulsen P, van Alphen L, ten Hove J, Fransen F, van der Ley P, Tommassen J. 2003. A Neisserial autotransporter NalP modulating the processing of other autotransporters. *Mol Microbiol* 50:1017–1030. <https://doi.org/10.1046/j.1365-2958.2003.03773.x>.
- Turner DP, Marietou AG, Johnston L, Ho KK, Rogers AJ, Wooldridge KG, Ala'Aldeen DA. 2006. Characterization of MspA, an immunogenic auto-transporter protein that mediates adhesion to epithelial and endothelial cells in *Neisseria meningitidis*. *Infect Immun* 74:2957–2964. <https://doi.org/10.1128/IAI.74.5.2957-2964.2006>.
- Oldfield NJ, Bland SJ, Taraktoglou M, Dos Ramos FJ, Robinson K, Wooldridge KG, Ala'Aldeen DA. 2007. T-cell stimulating protein A (TspA) of *Neisseria meningitidis* is required for optimal adhesion to human cells. *Cell Microbiol* 9:463–478. <https://doi.org/10.1111/j.1462-5822.2006.00803.x>.
- Hung MC, Heckels JE, Christodoulides M. 2013. The adhesin complex protein (ACP) of *Neisseria meningitidis* is a new adhesin with vaccine potential. *mBio* 4:e00041-13. <https://doi.org/10.1128/mBio.00041-13>.
- Fletcher LD, Bernfield L, Barniak V, Farley JE, Howell A, Knauf M, Ooi P, Smith RP, Weise P, Wetherell M, Xie X, Zagursky R, Zhang Y, Zlotnick GW. 2004. Vaccine potential of the *Neisseria meningitidis* 2086 lipoprotein. *Infect Immun* 72:2088–2100. <https://doi.org/10.1128/IAI.72.4.2088-2100.2004>.
- Schoen C, Tettelin H, Parkhill J, Frosch M. 2009. Genome flexibility in *Neisseria meningitidis*. *Vaccine* 27(Suppl 2):B103–B111. <https://doi.org/10.1016/j.vaccine.2009.04.064>.
- Marri PR, Paniscus M, Weyand NJ, Rendon MA, Calton CM, Hernandez DR, Higashi DL, Sodergren E, Weinstock GM, Rounsley SD, So M. 2010. Genome sequencing reveals widespread virulence gene exchange among human *Neisseria* species. *PLoS One* 5:e11835. <https://doi.org/10.1371/journal.pone.0011835>.
- Dunning Hotopp JC, Grifantini R, Kumar N, Tzeng YL, Fouts D, Frigimelica E, Draghi M, Giuliani MM, Rappuoli R, Stephens DS, Grandi G, Tettelin H. 2006. Comparative genomics of *Neisseria meningitidis*: core genome, islands of horizontal transfer and pathogen-specific genes. *Microbiology* 152:3733–3749. <https://doi.org/10.1099/mic.0.29261-0>.
- Joseph B, Schwarz RF, Linke B, Blom J, Becker A, Claus H, Goesmann A, Frosch M, Muller T, Vogel U, Schoen C. 2011. Virulence evolution of the human pathogen *Neisseria meningitidis* by recombination in the core and accessory genome. *PLoS One* 6:e18441. <https://doi.org/10.1371/journal.pone.0018441>.
- Hill DJ, Griffiths NJ, Borodina E, Virji M. 2010. Cellular and molecular biology of *Neisseria meningitidis* colonization and invasive disease. *Clin Sci (Lond)* 118:547–564. <https://doi.org/10.1042/CS20090513>.
- Coureuril M, Join-Lambert O, Lecuyer H, Bourdoulous S, Marullo S, Nassif X. 2013. Pathogenesis of meningococemia. *Cold Spring Harb Perspect Med* 3:a012393. <https://doi.org/10.1101/cshperspect.a012393>.
- Eisenreich W, Dandekar T, Heesemann J, Goebel W. 2010. Carbon metabolism of intracellular bacterial pathogens and possible links to virulence. *Nat Rev Microbiol* 8:401–412. <https://doi.org/10.1038/nrmicro2351>.
- Abu Kwaik Y, Bumann D. 2013. Microbial quest for food *in vivo*: 'nutritional virulence' as an emerging paradigm. *Cell Microbiol* 15:882–890. <https://doi.org/10.1111/cmi.12138>.
- Zhang YJ, Rubin EJ. 2013. Feast or famine: the host-pathogen battle over amino acids. *Cell Microbiol* 15:1079–1087. <https://doi.org/10.1111/cmi.12140>.
- Neumann W, Hadley RC, Nolan EM. 2017. Transition metals at the host-pathogen interface: how *Neisseria* exploit human metalloproteins for acquiring iron and zinc. *Essays Biochem* 61:211–223. <https://doi.org/10.1042/EBC20160084>.
- Weinberg ED. 1975. Nutritional immunity. Host's attempt to withhold iron from microbial invaders. *JAMA* 231:39–41. <https://doi.org/10.1001/jama.1975.03240130021018>.
- Cornelissen CN. 13 October 2017. Subversion of nutritional immunity by the pathogenic *Neisseriae*. *Pathog Dis* <https://doi.org/10.1093/femspd/ftx112>.
- Catlin BW. 1973. Nutritional profiles of *Neisseria gonorrhoeae*, *Neisseria meningitidis*, and *Neisseria lactamica* in chemically defined media and the use of growth requirements for gonococcal typing. *J Infect Dis* 128:178–194. <https://doi.org/10.1093/infdis/128.2.178>.
- Monaco C, Tala A, Spinosa MR, Progida C, De Nitto E, Gaballo A, Bruni CB, Bucci C, Alifano P. 2006. Identification of a meningococcal L-glutamate ABC transporter operon essential for growth in low-sodium environments. *Infect Immun* 74:1725–1740. <https://doi.org/10.1128/IAI.74.3.1725-1740.2006>.
- Takahashi H, Kim KS, Watanabe H. 2011. Meningococcal internalization into human endothelial and epithelial cells is triggered by the influx of extracellular L-glutamate via GltT L-glutamate ABC transporter in *Neisseria meningitidis*. *Infect Immun* 79:380–392. <https://doi.org/10.1128/IAI.00497-10>.
- Takahashi H, Yanagisawa T, Kim KS, Yokoyama S, Ohnishi M. 2015. Multiple functions of glutamate uptake via meningococcal GltT-GltM L-glutamate ABC transporter in *Neisseria meningitidis* internalization into human brain microvascular endothelial cells. *Infect Immun* 83:3555–3567. <https://doi.org/10.1128/IAI.00654-15>.
- Tala A, Monaco C, Nagorska K, Exley RM, Corbett A, Zychlinsky A, Alifano P, Tang CM. 2011. Glutamate utilization promotes meningococcal survival *in vivo* through avoidance of the neutrophil oxidative burst. *Mol Microbiol* 81:1330–1342. <https://doi.org/10.1111/j.1365-2958.2011.07766.x>.
- Colicchio R, Ricci S, Lamberti F, Pagliarulo C, Pagliuca C, Braione V, Braccini T, Tala A, Montanaro D, Tripodi S, Cintorino M, Troncone G, Bucci C, Pozzi G, Bruni CB, Alifano P, Salvatore P. 2009. The meningococcal ABC-type L-glutamate transporter GltT is necessary for the development of experimental meningitis in mice. *Infect Immun* 77:3578–3587. <https://doi.org/10.1128/IAI.01424-08>.
- Port JL, DeVoe IW, Archibald FS. 1984. Sulphur acquisition by *Neisseria meningitidis*. *Can J Microbiol* 30:1453–1457. <https://doi.org/10.1139/m84-232>.

37. Roupael NG, Stephens DS. 2012. *Neisseria meningitidis*: biology, microbiology, and epidemiology. *Methods Mol Biol* 799:1–20. https://doi.org/10.1007/978-1-61779-346-2_1.
38. Takahashi H, Hirose K, Watanabe H. 2004. Necessity of meningococcal γ -glutamyl aminopeptidase for the *Neisseria meningitidis* growth in rat cerebrospinal fluid (CSF) and CSF mimicking medium. *J Bacteriol* 186:244–247. <https://doi.org/10.1128/JB.186.1.244-247.2004>.
39. van de Waterbeemd B, Zomer G, van den Ijssel J, van Keulen L, Eppink MH, van der Ley P, van der Pol LA. 2013. Cysteine depletion causes oxidative stress and triggers outer membrane vesicle release by *Neisseria meningitidis*; implications for vaccine development. *PLoS One* 8:e54314. <https://doi.org/10.1371/journal.pone.0054314>.
40. Baart GJ, Zomer B, de Haan A, van der Pol LA, Beuvery EC, Tramper J, Martens DE. 2007. Modeling *Neisseria meningitidis* metabolism: from genome to metabolic fluxes. *Genome Biol* 8:R136. <https://doi.org/10.1186/gb-2007-8-7-r136>.
41. Schoen C, Kischkies L, Elias J, Ampattu BJ. 2014. Metabolism and virulence in *Neisseria meningitidis*. *Front Cell Infect Microbiol* 4:114. <https://doi.org/10.3389/fcimb.2014.00114>.
42. Takahashi H, Carlson RW, Muszynski A, Choudhury B, Kim KS, Stephens DS, Watanabe H. 2008. Modification of lipooligosaccharide with phosphoethanolamine by LptA in *Neisseria meningitidis* enhances meningococcal adhesion to human endothelial and epithelial cells. *Infect Immun* 76:5777–5789. <https://doi.org/10.1128/IAI.00676-08>.
43. Takahashi H, Yanagisawa T, Kim KS, Yokoyama S, Ohnishi M. 2012. Meningococcal PilV potentiates *Neisseria meningitidis* type IV pilus-mediated internalization into human endothelial and epithelial cells. *Infect Immun* 80:4154–4166. <https://doi.org/10.1128/IAI.00423-12>.
44. Carbonnelle E, Hill DJ, Morand P, Griffiths NJ, Bourdoulous S, Murillo I, Nassif X, Virji M. 2009. Meningococcal interactions with the host. *Vaccine* 27(Suppl 2):B78–B89. <https://doi.org/10.1016/j.vaccine.2009.04.069>.
45. Sa ECC, Griffiths NJ, Virji M. 2010. *Neisseria meningitidis* Opc invasin binds to the sulphated tyrosines of activated vitronectin to attach to and invade human brain endothelial cells. *PLoS Pathog* 6:e1000911. <https://doi.org/10.1371/journal.ppat.1000911>.
46. Kuespert K, Roth A, Hauck CR. 2011. *Neisseria meningitidis* has two independent modes of recognizing its human receptor CEACAM1. *PLoS One* 6:e14609. <https://doi.org/10.1371/journal.pone.0014609>.
47. Coureuil M, Lecuyer H, Bourdoulous S, Nassif X. 2017. A journey into the brain: insight into how bacterial pathogens cross blood-brain barriers. *Nat Rev Microbiol* 15:149–159. <https://doi.org/10.1038/nrmicro.2016.178>.
48. Lu SC. 2013. Glutathione synthesis. *Biochim Biophys Acta* 1830:3143–3153. <https://doi.org/10.1016/j.bbagen.2012.09.008>.
49. Hassett DJ, Cohen MS. 1989. Bacterial adaptation to oxidative stress: implications for pathogenesis and interaction with phagocytic cells. *FASEB J* 3:2574–2582. <https://doi.org/10.1096/fasebj.3.14.2556311>.
50. Ali S, Jain SK, Abdulla M, Athar M. 1996. Paraquat induced DNA damage by reactive oxygen species. *Biochem Mol Biol Int* 39:63–67.
51. Soler-García AA, Jerse AE. 2004. A *Neisseria gonorrhoeae* catalase mutant is more sensitive to hydrogen peroxide and paraquat, an inducer of toxic oxygen radicals. *Microb Pathog* 37:55–63. <https://doi.org/10.1016/j.micpath.2004.04.007>.
52. Alkhuder K, Meibom KL, Dubail I, Dupuis M, Charbit A. 2009. Glutathione provides a source of cysteine essential for intracellular multiplication of *Francisella tularensis*. *PLoS Pathog* 5:e1000284. <https://doi.org/10.1371/journal.ppat.1000284>.
53. Sprenger M, Kasper L, Dupuis M, Hube B. 7 November 2017. Metabolic adaptation of intracellular bacteria and fungi to macrophages. *Int J Med Microbiol* <https://doi.org/10.1016/j.ijmm.2017.11.001>.
54. Brosnan JT, Brosnan ME. 2006. The sulfur-containing amino acids: an overview. *J Nutr* 136:1636S–1640S. <https://doi.org/10.1093/jn/136.6.1636S>.
55. Stipanuk MH, Ueki I. 2011. Dealing with methionine/homocysteine sulfur: cysteine metabolism to taurine and inorganic sulfur. *J Inher Metab Dis* 34:17–32. <https://doi.org/10.1007/s10545-009-9006-9>.
56. Yin J, Ren W, Yang G, Duan J, Huang X, Fang R, Li C, Li T, Yin Y, Hou Y, Kim SW, Wu G. 2016. L-Cysteine metabolism and its nutritional implications. *Mol Nutr Food Res* 60:134–146. <https://doi.org/10.1002/mnfr.201500031>.
57. Ewann F, Hoffman PS. 2006. Cysteine metabolism in *Legionella pneumophila*: characterization of an L-cysteine-utilizing mutant. *Appl Environ Microbiol* 72:3993–4000. <https://doi.org/10.1128/AEM.00684-06>.
58. Muller A, Thomas GH, Horler R, Brannigan JA, Blagova E, Levdikov VM, Fogg MJ, Wilson KS, Wilkinson AJ. 2005. An ATP-binding cassette-type cysteine transporter in *Campylobacter jejuni* inferred from the structure of an extracytoplasmic solute receptor protein. *Mol Microbiol* 57:143–155. <https://doi.org/10.1111/j.1365-2958.2005.04691.x>.
59. Suginaka K, Yamamoto K, Ashiida H, Kono Y, Saw Y, Shibata H. 1998. Cysteine uptake for accumulation of glutathione by the *Cyanobacterium Synechocystis* strain PCC 6803. *Biosci Biotechnol Biochem* 62:424–428. <https://doi.org/10.1271/bbb.62.424>.
60. Méndez J, Reimundo P, Pérez-Pascual D, Navais R, Gómez E, Guisjarro JA. 2011. A novel *cdsAB* operon is involved in the uptake of L-cysteine and participates in the pathogenesis of *Yersinia ruckeri*. *J Bacteriol* 193:944–951. <https://doi.org/10.1128/JB.01058-10>.
61. Rusniok C, Vallenet D, Floquet S, Ewles H, Mouze-Soulama C, Brown D, Lajus A, Buchrieser C, Medigue C, Glaser P, Pelicic V. 2009. NeMeSys: a biological resource for narrowing the gap between sequence and function in the human pathogen *Neisseria meningitidis*. *Genome Biol* 10:R110. <https://doi.org/10.1186/gb-2009-10-10-r110>.
62. Ampattu BJ, Hagmann L, Liang C, Dittrich M, Schluter A, Blom J, Krol E, Goesmann A, Becker A, Dandekar T, Muller T, Schoen C. 2017. Transcriptional buffering of cryptic genetic variation contributes to meningococcal virulence. *BMC Genomics* 18:282. <https://doi.org/10.1186/s12864-017-3616-7>.
63. Takahashi H, Kim KS, Watanabe H. 2008. Differential *in vitro* infectious abilities of two common Japan-specific sequence-type (ST) clones of disease-associated ST-2032 and carrier-associated ST-2046 *Neisseria meningitidis* strains in human endothelial and epithelial cell lines. *FEMS Immunol Med Microbiol* 52:36–46. <https://doi.org/10.1111/j.1574-695X.2007.00342.x>.
64. Niu H, Xiong Q, Yamamoto A, Hayashi-Nishino M, Rikihisa Y. 2012. Autophagosomes induced by a bacterial Beclin 1 binding protein facilitate obligatory intracellular infection. *Proc Natl Acad Sci U S A* 109:20800–20807. <https://doi.org/10.1073/pnas.1218674109>.
65. Afzal M, Manzoor I, Kuipers OP, Shafeeq S. 2016. Cysteine-mediated gene expression and characterization of the CmbR regulon in *Streptococcus pneumoniae*. *Front Microbiol* 7:1929. <https://doi.org/10.3389/fmicb.2016.01929>.
66. Lindholm B, Alvestrand A, Furst P, Bergstrom J. 1989. Plasma and muscle free amino acids during continuous ambulatory peritoneal dialysis. *Kidney Int* 35:1219–1226. <https://doi.org/10.1038/ki.1989.113>.
67. Santangelo F. 2002. The regulation of sulphurated amino acid junctions: fact or fiction in the field of inflammation? *Amino Acids* 23:359–365. <https://doi.org/10.1007/s00726-002-0206-y>.
68. Su L, Li H, Xie A, Liu D, Rao W, Lan L, Li X, Li F, Xiao K, Wang H, Yan P, Li X, Xie L. 2015. Dynamic changes in amino acid concentration profiles in patients with sepsis. *PLoS One* 10:e0121933. <https://doi.org/10.1371/journal.pone.0121933>.
69. Zheng Y, Ritzenthaler JD, Burke TJ, Otero J, Roman J, Watson WH. 2018. Age-dependent oxidation of extracellular cysteine/cystine redox state (Eh(Cys/CySS)) in mouse lung fibroblasts is mediated by a decline in Slc7a11 expression. *Free Radic Biol Med* 118:13–22. <https://doi.org/10.1016/j.freeradbiomed.2018.02.026>.
70. Franco R, Schoneveld OJ, Pappa A, Panayiotidis MI. 2007. The central role of glutathione in the pathophysiology of human diseases. *Arch Physiol Biochem* 113:234–258. <https://doi.org/10.1080/13813450701661198>.
71. Tzeng YL, Thomas J, Stephens DS. 2016. Regulation of capsule in *Neisseria meningitidis*. *Crit Rev Microbiol* 42:759–772.
72. Ayala-Castro C, Saini A, Outten FW. 2008. Fe-S cluster assembly pathways in bacteria. *Microbiol Mol Biol Rev* 72:110–125, table of contents. <https://doi.org/10.1128/MMBR.00034-07>.
73. Takumi K, Nonaka G. 2016. Bacterial cysteine-inducible cysteine resistance systems. *J Bacteriol* 198:1384–1392. <https://doi.org/10.1128/JB.01039-15>.
74. Denk D, Bock A. 1987. L-Cysteine biosynthesis in *Escherichia coli*: nucleotide sequence and expression of the serine acetyltransferase (*cysE*) gene from the wild-type and a cysteine-excreting mutant. *J Gen Microbiol* 133:515–525. <https://doi.org/10.1099/00221287-133-3-515>.
75. Awano N, Wada M, Mori H, Nakamori S, Takagi H. 2005. Identification and functional analysis of *Escherichia coli* cysteine desulfhydrases. *Appl Environ Microbiol* 71:4149–4152. <https://doi.org/10.1128/AEM.71.7.4149-4152.2005>.
76. Locher HH, Schlunegger H, Hartman PG, Angehrn P, Then RL. 1996. Antibacterial activities of epiroprim, a new dihydrofolate reductase inhibitor, alone and in combination with dapson. *Antimicrob Agents Chemother* 40:1376–1381. <https://doi.org/10.1128/AAC.40.6.1376>.
77. Pintor M, Ferron L, Gomez JA, Powell NB, Ala'Aldeen DA, Borriello SP,

- Criado MT, Ferreiros CM. 1996. Blocking of iron uptake from transferrin by antibodies against the transferrin binding proteins in *Neisseria meningitidis*. *Microb Pathog* 20:127–139. <https://doi.org/10.1006/mpat.1996.0012>.
78. Takahashi H, Watanabe H. 2002. A broad-host-range vector of incompatibility group Q can work as a plasmid vector in *Neisseria meningitidis*: a new genetical tool. *Microbiology* 148:229–236. <https://doi.org/10.1099/00221287-148-1-229>.
79. Stark MJ. 1987. Multicopy expression vectors carrying the *lac* repressor gene for regulated high-level expression of genes in *Escherichia coli*. *Gene* 51:255–267. [https://doi.org/10.1016/0378-1119\(87\)90314-3](https://doi.org/10.1016/0378-1119(87)90314-3).
80. Motohashi K. 2015. A simple and efficient seamless DNA cloning method using SLiCE from *Escherichia coli* laboratory strains and its application to SLiP site-directed mutagenesis. *BMC Biotechnol* 15:47. <https://doi.org/10.1186/s12896-015-0162-8>.
81. Takahashi H, Watanabe H. 2004. Post-translational processing of *Neisseria meningitidis* γ -glutamyl aminopeptidase and its association with inner membrane facing to the cytoplasmic space. *FEMS Microbiol Lett* 234:27–35. <https://doi.org/10.1016/j.femsle.2004.03.003>.
82. Takahashi H, Watanabe H. 2005. A gonococcal homologue of meningococcal γ -glutamyl transpeptidase gene is a new type of bacterial pseudogene that is transcriptionally active but phenotypically silent. *BMC Microbiol* 5:56. <https://doi.org/10.1186/1471-2180-5-56>.
83. Sa ECC, Griffiths NJ, Murillo I, Virji M. 2009. *Neisseria meningitidis* Opc invasin binds to the cytoskeletal protein alpha-actinin. *Cell Microbiol* 11:389–405. <https://doi.org/10.1111/j.1462-5822.2008.01262.x>.
84. Hassett DJ, Britigan BE, Svendsen T, Rosen GM, Cohen MS. 1987. Bacteria form intracellular free radicals in response to paraquat and streptonigrin. Demonstration of the potency of hydroxyl radical. *J Biol Chem* 262: 13404–13408.
85. Tseng HJ, Srikhanta Y, McEwan AG, Jennings MP. 2001. Accumulation of manganese in *Neisseria gonorrhoeae* correlates with resistance to oxidative killing by superoxide anion and is independent of superoxide dismutase activity. *Mol Microbiol* 40:1175–1186. <https://doi.org/10.1046/j.1365-2958.2001.02460.x>.
86. Seib KL, Jennings MP, McEwan AG. 2003. A Sco homologue plays a role in defence against oxidative stress in pathogenic *Neisseria*. *FEBS Lett* 546:411–415. [https://doi.org/10.1016/S0014-5793\(03\)00632-X](https://doi.org/10.1016/S0014-5793(03)00632-X).
87. Wu HJ, Seib KL, Edwards JL, Apicella MA, McEwan AG, Jennings MP. 2005. Azurin of pathogenic *Neisseria* spp. is involved in defense against hydrogen peroxide and survival within cervical epithelial cells. *Infect Immun* 73: 8444–8448. <https://doi.org/10.1128/IAI.73.12.8444-8448.2005>.